



Cite this: *Lab Chip*, 2025, 25, 1097

## Challenges in blood fractionation for cancer liquid biopsy: how can microfluidics assist?†

Robert Salomon, <sup>\*ab</sup> Sajad Razavi Bazaz, <sup>a</sup> Kirk Mutafopoulos, <sup>c</sup> David Gallego-Ortega, <sup>bdef</sup> Majid Warkiani, <sup>be</sup> David Weitz <sup>c</sup> and Dayong Jin <sup>b</sup>

Liquid biopsy provides a minimally invasive approach to characterise the molecular and phenotypic characteristics of a patient's individual tumour by detecting evidence of cancerous change in readily available body fluids, usually the blood. When applied at multiple points during the disease journey, it can be used to monitor a patient's response to treatment and to personalise clinical management based on changes in disease burden and molecular findings. Traditional liquid biopsy approaches such as quantitative PCR, have tended to look at only a few biomarkers, and are aimed at early detection of disease or disease relapse using predefined markers. With advances in the next generation sequencing (NGS) and single-cell genomics, simultaneous analysis of both circulating tumour DNA (ctDNA) and circulating tumour cells (CTCs) is now a real possibility. To realise this, however, we need to overcome issues with current blood collection and fractionation processes. These include overcoming the need to add a preservative to the collection tube or the need to rapidly send blood tubes to a centralised processing lab with the infrastructure required to fractionate and process the blood samples. This review focuses on outlining the current state of liquid biopsy and how microfluidic blood fractionation tools can be used in cancer liquid biopsy. We describe microfluidic devices that can separate plasma for ctDNA analysis, and devices that are important in isolating the cellular component(s) in liquid biopsy, *i.e.*, individual CTCs and CTC clusters. To facilitate a better understanding of these devices, we propose a new categorisation system based on how these devices operate. The three categories being 1) solid Interaction devices, 2) fluid Interaction devices and 3) external force/active devices. Finally, we conclude that whilst some assays and some cancers are well suited to current microfluidic techniques, new tools are necessary to support broader, clinically relevant multiomic workflows in cancer liquid biopsy.

Received 3rd July 2024,  
Accepted 14th November 2024

DOI: 10.1039/d4lc00563e

rsc.li/loc

### 1. Importance of liquid biopsy

Liquid biopsy provides a unique opportunity to characterise individual cancers and to understand a patient's unique disease and response to treatment. By identifying cells and/or cell products that are associated with cancer in the blood of patients, it is possible to detect the presence of even low disease burden without the need to biopsy the tumour or to

anatomically locate the metastatic lesions. Although originally designed to allow detection of cancer, the role of liquid biopsy has expanded and now has application in altering treatment plans based on the patient's own molecular profile. For this reason, it is set to become an important test in the application of precision genomic medicine.

Liquid biopsy has traditionally targeted 3 main biological targets. These include: 1) protein biomarkers 2) circulating tumour DNA (ctDNA) and 3) circulating tumour cells (CTCs). In addition, small extracellular vesicles, CTC clusters and lipids are becoming important targets for liquid biopsy. More details on the common liquid biopsy analytes can be found in Box 1. Whilst these analytes can be found in various body fluids (including cerebrospinal fluid (CSF), ascites, saliva, urine, *etc.*) liquid biopsy traditionally relies on detecting these targets in peripheral blood. This reliance likely stems from the fact that the peripheral blood system is readily available, can be assessed with minimal risk to the patient, and blood draws are a common procedure routinely done without the need for surgical intervention (unlike sampling of CSF, bone

<sup>a</sup> Children's Cancer Institute, Lowy Cancer Research Centre, UNSW, Sydney, Australia. E-mail: rsalomon@ccia.org.au

<sup>b</sup> Institute for Biomedical Materials and Devices (IBMD)/Faculty of Science, University of Technology Sydney, Sydney, NSW, 2007 Australia

<sup>c</sup> Department of Physics, Harvard University, Cambridge, MA, 02138, USA

<sup>d</sup> School of Clinical Medicine, Faculty of Medicine, University of New South Wales, Sydney, NSW, 2052, Australia

<sup>e</sup> School of Biomedical Engineering, University of Technology Sydney, Sydney, New South Wales 2007, Australia

<sup>f</sup> Garvan Institute of Medical Research, Darlinghurst, Sydney, NSW 2010, Australia

† Electronic supplementary information (ESI) available. See DOI: <https://doi.org/10.1039/d4lc00563e>



marrow, and ascites which are more invasive and less common routes for liquid biopsy).

### Box 1 Common analytes in cancer related liquid biopsy

Protein biomarkers such as PSA<sup>1</sup> and a host of serum antigens<sup>2</sup> formed the base of some of the earliest liquid biopsy approaches in cancer. Many of these proteins are not solely expressed by cancer, and thus additional confirmation tests are required to confirm a cancer diagnosis.

Circulating tumour DNA (ctDNA) is a subset of cell free DNA that contains cancer specific mutational changes. Since at least 1996, ctDNA profiles have been identified in the blood of patients with cancer.<sup>3,4</sup> The identification of mutational change in ctDNA is commonly used to detect disease, identify the molecular subtype of disease and studies have indicated that changes in ctDNA levels may be prognostic of outcome.<sup>5,6</sup> As ctDNA potentially originates from any tumour cell, it can be thought of as a measure of total tumour burden.

Circulating tumour cells (CTCs) are cancer cells that can be found in the circulation. For solid tumours they are a subset of disseminated tumour cells (DTCs) that have found their way out of the confines of either the primary or metastatic lesion but have not yet completed the process of metastatic spread. As CTCs are the primary route by which cancer spreads, they can be thought of as measure of potential metastasis.

Small extracellular vesicles are small lipid particles 30–150 nm<sup>7</sup> which are thought to carry key cell signalling messages. Whilst beyond the scope of this review, more details relating to microfluidic approaches to small extracellular vesicle capture can be readily found.<sup>8–10</sup>

CTC clusters consist of one or more CTCs and may form clusters with either other CTCs or “normal” cells and are increasingly being recognised as important players in the metastatic cascade.<sup>11–14</sup>

Lipids form a diverse range of biomolecules including fats, phospholipids and steroids. They have been implicated in early diagnosis and monitoring of cancer in a number of studies.<sup>15,16</sup>

While early liquid biopsy tended to focus on detection of a single marker or basic CTC enumeration, the field of liquid biopsy is now able to shed light on many important clinical questions. Modern liquid biopsy has important application in the early detection of disease,<sup>17–19</sup> assessing cancer heterogeneity,<sup>20,21</sup> and determining molecular drivers of disease.<sup>22</sup> When applied longitudinally, it can help determine relapse, monitor resistance to therapy,<sup>23,24</sup> and assess clonal evolution.<sup>24–26</sup> Moreover, as liquid biopsy can readily be repeated throughout the patient's disease journey, it can be used to dynamically inform treatment options.<sup>27–29</sup>

## 2. Next generation liquid biopsy

With the advent of affordable low input next-generation sequencing (NGS), it became possible to not only detect disease, but to sequence the underlying genetic

abnormalities seen in a cancer patient by interrogating at cell free DNA (cfDNA) in the plasma. This meant the ctDNA could either be interrogated agnostically by analysing the entire genomic profile using whole genome sequencing (WGS)<sup>30</sup> or specifically through the use of targeted NGS panels. These panels can either be designed to include genetic variants common across a number of patients or constructed against the unique molecular profile of the individual patient to deeply sequence a smaller number of high value gene targets.<sup>31</sup>

WGS approaches were initially applied at relatively low sequencing depth. Sequencing depths as low as ~0.4× or 0.6× genome coverage have been shown to be able to detect disease.<sup>32,33</sup> However, by sequencing further (6× to 8× genome coverage), it is possible to look at the tissue of origin for the cancer in a process involving fragmentomics (see reviews<sup>34,35</sup>). These approaches are unlikely to capture every individual mutation. Therefore, low coverage WGS approaches are more suitable for tumours which tend to have a high tumour mutation burden (TMB) (as more potential targets exist) or in diseases characterised by copy number aberrations (CNAs). For tumours not characterised by CNAs or high TMBs, low pass WGS has limited application, and it can be useful to apply targeted panels. Targeted panels come in two forms: pan-cancer panels and personalised panels. Pan-cancer panels, such as the Trusight Oncology 500 ctDNA from Illumina or the Xgen Pan-Cancer hybridisation panel from IDT, are useful as they cover many of the commonly mutated cancer genes. In cancer types with well conserved genetic changes across many patients, it is possible to design cohort specific panels, such as the UltraSEEK lung Panel. These panels focus on reducing the number of probes required without the additional cost of sequencing regions unlikely to be mutated. When a disease cohort is highly heterogeneous and where genetic mutations are not shared amongst multiple patients, two approaches can be enacted to enable sufficient detection sensitivity. The first approach requires a large pool of targets, such that can be achieved using whole exome sequencing or with very large capture/amplicon panels, whilst the second approach relies on knowing which targets are present in the patient's own tumour. This approach is truly personalised and whilst it reduces liquid biopsy sequencing costs, it requires the patient's tumour to be sequenced in advance.

Larger, multiple target panels, such as those identified using the INVAR approach,<sup>31</sup> work as they increase the chance of detecting mutations by including more detection options, while personalised panels work by heavily preselecting targets that have an increased likelihood of being found in the patient's own tumour. The issue with large panels is primarily around cost while the problem with personalised panels is the need to have *a priori* knowledge of the individual's cancer genome. Studies such as the TRACER X,<sup>36</sup> PROPHET,<sup>37</sup> and others<sup>38–40</sup> are excellent examples of where personalised ctDNA panels have been effectively applied.



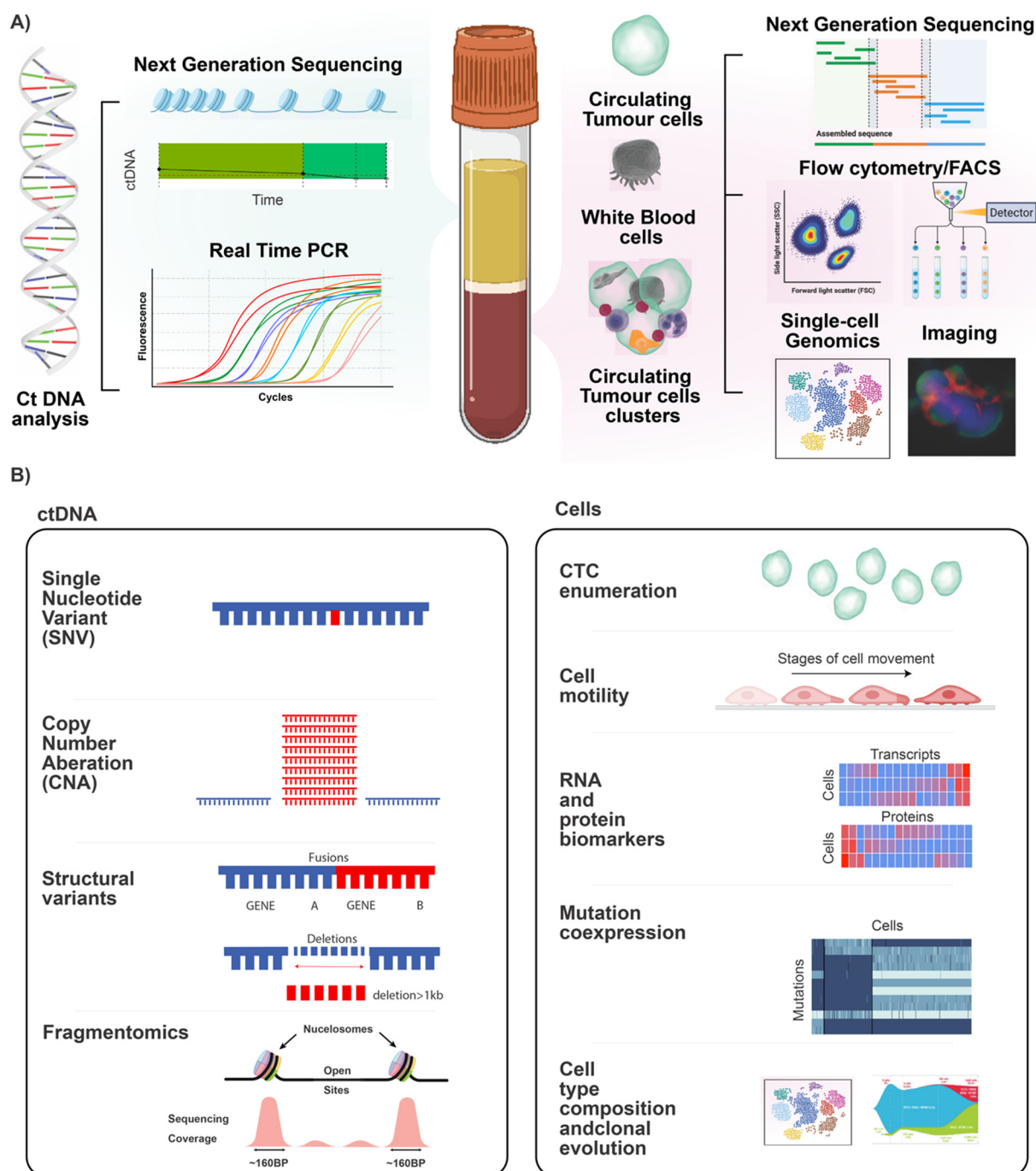


**Fig. 1** Key components of the peripheral blood and how they are leveraged into cancer liquid biopsy applications. A) Shows the components found within the blood that can be used in cancer liquid biopsy. On the left-hand side is the ctDNA which is found in the plasma and can be analysed using molecular approaches such as next generation sequencing and single target quantitative PCR. The right panel shows the cellular evidence for cancer, this includes CTCs, CTC clusters, and immune cells. These can be analysed using bulk genomic approaches, flow cytometry for analysis or FACS for associated cell sorting, and genomic cytometry/single cell genomics and imaging. B) Highlights the biologically relevant information that can be retrieved via characterisation of ctDNA and CTCs. Left panel: depending on the methods employed to analyse ctDNA it is possible to look at SNV and CNA profiles as well as structural variants. In addition, emerging approaches such as fragmentomics are allowing us to deconvolute the ctDNA to look at tissue of origin and other key metrics. Right panel: By using traditional cytometric approaches alongside single-cell genomics it is now possible to perform CTC enumeration, analyse CTC motility, perform deep phenotypic profiling (using RNA and oligo antibody approaches in scRNASeq), and look for mutational profiles in the single cells (via single-cell DNA sequencing). By using these molecular profiling techniques, it is also possible to perform detailed cell type profiling and to track clonal evolution.

Just as we have seen advances in NGS that have improved cancer liquid biopsy, advancements in cytometry and single-cell genomics analysis have exponentially increased the number of targets that can be simultaneously analysed at the single cell level.<sup>41–43</sup> This is important because, although detection of CTCs above a clinically relevant level (*e.g.* >5 CTCs ml<sup>-1</sup> in breast cancer) generally indicates poorer outcomes,<sup>44</sup> it does not provide certainty of disease outcome.<sup>45</sup> This finding suggests that metrics other than simple enumeration could provide more accurate prognosis. By taking advantage of the improvements in sensitivity, reduction in cost, and the capability to perform simultaneous multiomic analysis, the field of single cell sequencing and genomic cytometry is now making it possible to characterise cells in terms of DNA *i.e.* (single nucleotide variants (SNV),<sup>27,46</sup> copy number aberrations (CNA)<sup>23,47</sup>), RNA expression levels,<sup>20</sup> and epigenetic changes<sup>48–50</sup> of individual cells, including CTCs.<sup>51,52</sup> The ability to genetically profile CTCs is important, as by knowing both CTC burden and the molecular profile of the cells that may set up distant metastatic lesions, we will be better equipped to not only escalate or de-escalate treatment but also alter treatment in response to the detection of therapeutic resistance.

Whilst independently assessing ctDNA and CTC profiles in cancer has been powerful, multimodal profiling is promising to allow the simultaneous profiling of both the ctDNA and the CTCs from a single blood draw. If this can be effectively implemented, it will allow a more detailed picture of a patient's individual disease in the most minimally invasive manner and provide both a total tumour burden measure (from ctDNA) and the ability to look for active evidence of metastatic spread (CTCs). As cancer is a complex disease, the rationale is that the more information that can be garnered from a single blood draw, the better we can assess and treat the patient.

### 3. Challenges in blood fractionation and cancer liquid biopsy

The first step in any liquid biopsy assay is to separate assay targets (such as ctDNA and CTCs) from the complex mixture in which they are found. In the case of ctDNA, the first step is to obtain pure cell-free plasma, while for CTCs, the first step is to debulk the cellular fraction without losing rare CTCs.

Blood is a complex mixture and contains two main components used in cancer liquid biopsy. These are the plasma and the cellular layer (buffy coat). Cell Free DNA (cfDNA), which contains ctDNA is found within the plasma fraction and can be subjected to assays such as next generation sequencing and quantitative PCR. The buffy coat contains the nucleated cells, including the CTCs, CTC cluster and immune cells. This layer can be subjected to analysis *via* bulk NGS, flow cytometry and fluorescent activated cell sorting (FACS), single cell genomics and imaging. A schematic of technologies related to the analysis of these

blood fractions is shown in Fig. 1A. Fig. 1B shows the types of information that can be gathered through further analysis of these fractions. Analysis of the cfDNA in the plasma allows the detection of genomic alterations such as single nucleotide polymorphisms, copy number aberrations, structural variants, and can even be analysed using fragmentomics to identify the tissue of origin for the tumour. Using cytometric approaches on the cell layer, it is possible to enumerate, visualise, and genetically characterise CTCs and other cell types. Importantly, it is possible to quantify the cellular co-expression of RNA, protein, DNA mutations at the level of the single cell, and to perform cell type composition analysis and to track clonal expansion. By analysing the blood of cancer patients, it is possible to 1) quantify levels of disease, 2) identify tissue of origin (see review of cell-free DNA fragmentomics<sup>53</sup>) and 3) isolate the molecular mechanism responsible for disease and particularly therapeutic resistance. This can be used to aid in identifying treatment options that are most likely to address the molecular alterations identified in the patient's individual cancer.

#### 3.1. ctDNA

Early work showing that cell-free DNA levels tend to be elevated in cancer patients was published in 1977.<sup>54</sup> Isolated ctDNA has been used to detect known mutations,<sup>55</sup> fusions,<sup>56</sup> copy number variations<sup>57</sup> and epigenetic profiles.<sup>58,59</sup> It has also been used to measure tumour burden in cancers including lung,<sup>24,37,57</sup> melanoma,<sup>17</sup> breast,<sup>26,60</sup> neuroblastoma,<sup>61</sup> pancreas,<sup>18</sup> prostate,<sup>62,63</sup> colon,<sup>64</sup> and colorectal.<sup>5,38</sup>

ctDNA fragments are found in the plasma fraction of the blood and are small DNA nucleic acid molecules around 160 base pairs in length. They are found alongside other cell-free DNA molecules that do not originate from the tumour and are often very rare. Therefore, there is a significant challenge in obtaining sufficient volume of plasma and cell-free DNA to reliably detect cancer at low levels.<sup>65</sup> As such it is critical to develop systems that provide high purity plasma with excellent recovery and can do this without allowing cellular breakdown and compromising the quality of the resulting plasma.

The challenges when dealing with ctDNA include:

1. Cell-free DNA (cfDNA) is found in both healthy individuals and those with cancer and whilst there is some evidence to suggest that patients with cancer may have elevated levels of cfDNA,<sup>66</sup> quantification of cfDNA alone is generally considered as having low diagnostic value.<sup>54</sup> Therefore, simple measurements of cfDNA are not sufficient, even for detection of cancer.

2. Clinically relevant ctDNA levels can be low (<1% of all cfDNA molecules in plasma). It is therefore important that all potential ctDNA molecules are captured.

3. ctDNA can be readily contaminated by cellular DNA *via* the introduction of high molecular weight genomic DNA



contamination from leukocyte lysis.<sup>67,68</sup> Therefore, samples must be processed quickly, or preservatives must be introduced to prevent WBC lysis.

4. To confirm if an individual has cancer, the cfDNA must be profiled and cfDNA containing mutations associated with cancer must be identified.<sup>69</sup> Therefore, highly efficient molecular pipelines are required.

### 3.2. CTCs

The existence of CTCs has been known since 1869 when Thomas Ashworth first described the existence of tumour-like cells in the blood of a patient.<sup>70</sup> Since then, many studies, mainly concerning epithelial cancers such as breast,<sup>44</sup> colorectal,<sup>64</sup> prostate,<sup>46</sup> kidney,<sup>71</sup> and lung<sup>72</sup> have highlighted the importance of CTCs. With the advent of new cell surface biomarkers and label free methods, the link between CTC levels and prognosis is becoming clearer for non-epithelial cancers. This includes brain cancer,<sup>73</sup> neuroblastoma,<sup>74</sup> and sarcoma.<sup>75</sup>

CTCs are important as they are the route through which cancer spreads and can provide a valuable window into a patient's individual disease, may help to assess tumour heterogeneity,<sup>76,77</sup> and overcome sampling issues associated with solid biopsies that may result in missing mutations associated with metastasis.<sup>46</sup> Clinically, CTC detection can allow earlier detection of disease when compared to imaging techniques,<sup>78</sup> and levels of CTCs can be prognostic of disease outcome.<sup>79,80</sup> In addition, there is strong evidence that CTCs can be used to track clonal evolution and dynamic heterogeneity, especially from haematological malignancy where CTC numbers can be high.

CTCs reside in the cellular component of the blood and are vastly outnumbered by red blood cells (RBCs). RBCs form the majority of the blood's cellular compartment<sup>81</sup> and are biconcave disks of 7.5 to 8.7  $\mu\text{m}$  in diameter and are 1.7 to 2.2  $\mu\text{m}$  thick.<sup>82</sup> Removal of the RBCs can be achieved with very small filters.<sup>83</sup> The requirement for pore sizes significantly smaller than the size of the RBC is due to the high deformability of RBCs which allows them to squeeze through passages smaller than their actual physical size.<sup>82</sup> In addition, devices designed to be used with whole blood must be capable of dealing with the very high concentrations of cells found in blood. This is a significant challenge as blood is normally composed of around 40–45% haematocrit, which translates to a cellular concentration comprising 4.8 to 5.31 billion ( $10^9$ ) red blood cells (RBCs), 5.8 to 7.44 million ( $10^6$ ) white blood cells (WBCs) and 230 to 285 million ( $10^6$ ) platelets per ml.<sup>81</sup>

The challenges when dealing with CTCs include:

1. CTCs are exceedingly rare cells with as little as 5 CTCs per ml of blood being clinically significant.<sup>44</sup> Therefore, every cell counts.
2. In addition to being rare, CTCs are generally overwhelmed ( $>1$  billion to one), by normal blood cells.

Therefore, systems must be capable of sorting large numbers of cells.

3. There is significant variation in CTC numbers based on disease type and stage. Estimates of CTC numbers in patients vary from zero to  $\sim 25\,000$  in 7.5 ml of blood.<sup>84</sup> Therefore, systems of capture must be able to handle anywhere from one CTC to several thousands of cells.

4. CTCs have a short half-life.<sup>85,86</sup> Therefore, CTC analysis should be performed as soon as possible after collection.

5. CTCs may be found as either individual cancer cells or as cell clusters, in which case they are known as CTC clusters. As CTC clusters can be composed of 2 or many cells, the system must be able to handle clusters of highly variable sizes.

6. In addition to forming clusters with other CTCs, CTCs may cluster with other cell types, including WBCs (heterotypic). Therefore, capture systems that rely on the depletion of WBCs (*i.e.*, through immunoaffinity methods) may deplete some CTC clusters.

7. The emerging acceptance of cancer-associated cells in the blood is also driving changes in the way blood needs to be processed for liquid biopsy. Immune profiling as part of liquid biopsy means that WBCs are no longer a waste product in liquid biopsy. Therefore, systems of capture must not create biases in the WBC populations.

8. CTC based separation overwhelmingly relies on the assumption that these cells either uniquely express a single cell surface marker or they are larger in size when compared to other cells. EMT transformation, the increasing recognition of CTC heterogeneity, and evidence pointing to the existence of small CTCs mean that existing methods may not capture all CTCs. Therefore, systems that use multiple CTC attributes may be more efficient at capturing all CTCs.

### 3.3. Conventional approaches to blood fractionation

Traditional blood fractionation approaches have generally relied on separation through either density or filtration-based discrimination. By centrifuging blood containing an anticoagulant at high speeds, a density gradient forms, and the blood separates into three distinct compartments. These fractions are: 1) the lighter plasma fraction, 2) the buffy coat cell fraction, and 3) the bottom RBC fraction. The drawback with the centrifugal-based approaches is that the interface between the layers can be difficult to accurately define and the choice of where to apply the cut off between the layers is left entirely to the operator.

With regards to plasma fractionation, inaccurate determination of the plasma and the cell layers can have the effect of both losing plasma (when not enough plasma is taken) or risk contamination of the cfDNA fraction (when part of the cellular layer is accidentally transferred with the plasma fraction and dying cells release high molecular weight DNA<sup>87</sup>). Although these issues can be minimised with operator training or with automation, this requires the development of expertise or the acquisition of expensive and



bulky liquid handling robotics and is generally not achievable outside of specialist labs.

To assist with separating the buffy coat cells from the RBC layer, density gradient media, such as Lymphoprep, Ficoll, Percoll®, and Histopaque®, have been developed. The use of density media can be further enhanced through specially designed tubes, such as SepMate™, PluriMate, leucosep, which are designed to help prevent the layers from mixing. Products, such as RosetteSep™ and HetaSep™, also incorporate the capacity to deplete unwanted cells. However, in cancer applications, all these methods are dependent on the target CTC's having a known density profile and only separate the major blood fractions. As such CTCs are still heavily contaminated with either RBCs, WBCs, or a combination of both and require further processing. Such methods usually include:

- RBC lysis is usually achieved using ammonium chloride. However, buoyancy (Akadeum human RBC depletion microbubbles) and microfluidic methods have also been developed.<sup>88</sup>

- Magnetic activated cell sorting (MACS).<sup>89</sup>
- Fluorescent activated cell sorting (FACS).<sup>90,91</sup>

Analysis of both ctDNA and CTCs to produce clinically relevant information is a non-trivial process. It requires close attention, not only to the specifics of the chosen analysis method but also to a host of pre-analytical variables including the way the sample is prepared.<sup>87,92–94</sup> Time is one of the major pre-analytical factors that can affect the results of liquid biopsy assays. This is related to the short half-lives of both ctDNA and CTCs and the fact that when non-cancer cells break down in the tube they will release normal DNA that can dilute the ctDNA signal. To minimise this, several blood collection tubes (BCTs), containing mostly proprietary preservatives have been developed and commercialised by companies such as Streck, Roche, ZYMO and Becton Dickinson. These tubes can be used to store blood at room temperature and allow up to 5 days between collection and processing without compromising cfDNA integrity.<sup>68,95</sup> However, the biggest challenge in using these BCTs in deep characterisation workflows lies in the fact that they significantly impact the quality of RNA for downstream applications and should only be used when ctDNA is the target.<sup>96</sup> Our own findings also show that these tubes significantly compromise the cytometric profiles. As such, it is currently recommended that multimodal analysis of ctDNA and CTC still relies on blood being collected into different BCTs.<sup>95,97</sup>

Processing blood samples for liquid biopsy using conventional approaches is currently far from routine and samples are often shipped to specialised laboratories for processing where automation and specialist wet lab staff are trained to process samples. An alternative approach to the use of BCTs containing preservatives and centralised processing is to use microfluidic blood fractionation at the point-of-draw. Due to the rarity of CTCs and the low abundance of ctDNA, an array of microfluidic approaches have been developed. This review focuses on microfluidics

devices that facilitate liquid biopsy for ctDNA and CTCs, how they work, where they fall short, and what would be required to advance genomic profiling of disease through minimally invasive blood tests.

## 4. Overcoming challenges, a role for microfluidics

Microfluidics is well suited as an approach to improve blood fractionation for cancer liquid biopsy. This is because it: 1) allows accurate manipulation of small sample volumes (especially important in paediatric liquid biopsy), 2) comes with low infrastructure costs (important for uptake in an already stretched healthcare system), 3) imparts minimal stress on the cells (minimal stress results in higher viability), 4) can be used without the need for complex labelling/handling protocols, and 5) are generally closed systems (making them low loss and safe to operate as no aerosols are created). Over the years, several different microfluidic approaches for fractionating blood into its various components have been developed and have previously been reviewed, particularly for CTCs.<sup>98–100</sup> However, there is still no consensus about which approach is best applied for which biological context, especially in the context of multiomic liquid biopsy.

Microfluidic plasma separation is commonly achieved *via* several methods, including 1) physical filtration, 2) plasma skimming *via* the Fareheus effect, 3) bifurcation or the Zweifach–Fung effect, 4) deterministic lateral displacement (DLD) (requires significant dilution of blood), 5) inertial focusing (requires significant dilution of blood), and 6) acoustophoresis. A description of the microfluidic devices available, their strengths, weakness and their working mechanism is provided in Table 1 (plasma separation).

CTC separation by microfluidics can be achieved with either passive or active methods, these commonly include 1) physical capture, 2) affinity surface capture, 3) deterministic lateral displacement (DLD), 4) acoustophoresis, 5) microfluidic magnetic associated cell separation (mMACS), 6) inertial separation and 7) microfluidic fluorescent activated cell sorting (mFACS). A description of the microfluidic devices available, their strengths, weaknesses, and their working mechanism is provided in Table 2 (CTC separation).

Despite the apparent complexity of microfluidic devices available, blood fractionation is generally achieved through separations based on either size/deformability or cell surface expression of protein. The mechanism of action can be used to separate these devices into three main categories. These groupings help to understand when and where an approach can be utilised, is based on the forces used to affect separation, and whether the cells are required to come into physical contact with the device. We propose that microfluidic devices for blood fractionation can be divided into three categories based on the working mechanism. These are:



Table 1 Overview of microfluidic devices for plasma separation

Device name	Target fraction	Year	Category	Mechanism and separation characteristic	Efficiency and purity	Speed or max volume	Chip complexity (1 is simple, 5 is complex)	Pre-processing and running buffers required	Reference
Planar microfilters	Plasma	2005	SI	Filtration Size	N/A N/A		4		101
DLD-PD	Plasma	2006	SI	DLD Size	100%	0.4 $\mu\text{l min}^{-1}$	3	No Yes	102
Zweifach-Fung	Plasma	2006	FI	Zweifach-Fung Size	15–25%	10 $\mu\text{l min}^{-1}$	4	N/A No	103
	Plasma	2016	FI	Zweifach-Fung Size	1–6% yield Residual contamination is 20 000 RBCs $\mu\text{L}^{-1}$ and ~80 WBCs $\mu\text{L}^{-1}$	0.5 $\text{ml min}^{-1}$	2	No No	104
	Plasma	2009	EF	Acoustophoresis	RBC contamination of $3.65 \times 10^9$ per litre	80 $\mu\text{l min}^{-1}$	4	No	105
Bead packed microchannels	Plasma	2010	SI	Filtration Size		20 $\mu\text{l}$ of whole blood	1		106
Contraction expansion arrays	Plasma	2011	FI	Inertial Size	62% yield 60% RBC rejection ratio	1.2 $\text{ml h}^{-1}$	1	10 $\times$ dilution Yes, running buffer required	107
Capillary driven, dielectrophoresis enabled microfluidic system	Plasma	2015	SI + EF	Filtration + dielectrophoresis Size		165 $\text{nl}$ of plasma extracted in 15 min	2	N/A No	108
	Plasma	2016	EF	Electrothermal flow		50 $\mu\text{l h}^{-1}$	5	10 $\times$ dilution	109
All-glass bifurcation microfluidic chip	Plasma	2017	FI	Bifurcation Size	74% (@25% haematocrit)	700 $\mu\text{l min}^{-1}$	2	2 $\times$ dilution No	110
Fully automated, on-site isolation of cfDNA	Plasma	2018	EF (LOD)	Centrifugation Buoyancy/density	Not disclosed	3 $\text{ml}$ in ~30 min to produce cfDNA	5 but simple to run	As this device is designed for automated cfDNA extraction many reagents are required	111
	Plasma	2020	SI	Filtration	71.7% yield @45% haematocrit	60 $\mu\text{l}$ in 6 min	3	No	112
				Size	RBC deletion of 99.8% and WBC depletion of 91.8%			No	
	Plasma	2022	SI	Filtration	50.3% to 88.5% of max plasma volume	50 $\mu\text{l}$ blood in 2 min	3	No	113
	Plasma	2010	FI	Size	Not disclosed			No	
	Plasma	2018	SI	Filtration + affinity capture Size + epitope expression	Up to 17.8% yields	100 $\mu\text{l min}^{-1}$	3	1:20 dilution No	114
					6 $\mu\text{l}$ whole blood at 0.3 $\mu\text{l min}^{-1}$	4	Yes, collected plasma is diluted at 0.76 $\times$	115	

## Solid interactions devices

This category relies on physical interactions to facilitate fractionation based on particle size. Whilst devices in this family can be quite distinct from one another, they all use physical interactions of the particles in blood to facilitate

fractionation. As blood components can vary in size from very small, such as exosomes 30–150 nm,<sup>7</sup> to very large CTC clusters consisting of many cells that can be up to 340  $\mu\text{m}$  in head and neck cancer,<sup>157</sup> this category of devices can be used to separate all components in the blood.



**Table 2** Overview of microfluidic devices for CTC separation

Device name	Target fraction	Year	Category	Mechanism and separation characteristic	Efficiency and purity	Sample speed or max volume	Chip complexity (1 is simple, 5 is complex)	Pre-processing and running buffers required	Reference
Integrated inertial ferrohydrodynamic cell separation (i2FCS)	CTC	2021	FI + EF	Inertial + mads	99.7%	60 ml h <sup>-1</sup> (2 × 10 <sup>5</sup> cells per s <sup>-1</sup> )	4	Cell staining and RBC lysis	116
Cluster-wells	CTC clusters	2022	SI	Filtration Size and epitope expression (CD4/16/66b/3 depletion)	4.07-log depletion, removing 99.992% of leukocytes	LNCAP: 100% 6 or more cells, ~98.7% of 5-cell clusters, dropping to ~75.8% of LNCAP doublets	25 ml h <sup>-1</sup>	4 but simple to run	Sample resuspended in ferrofluid and pluronic F-68 surfactant 117
Continuous centrifugal microfluidics (CCM)	ctDNA and CTC	2022	EF (LOD)	Centrifugal + MACS CD45 depletion	<0.06% WBC <0.025% platelet contamination ~80% depending on cell line WBCs depletion >99%	5.4 ml whole blood	5 but simple to run	No pre-filling of density gradient media and antiCD45 MACS beads required 118	118
Spiral-contraction-expansion channel	CTC and CTC clusters	2024	FI	Inertial Size	97% MDAMB-231 and 90% CTC clusters WBC contamination is 31% in CTCs and 87% CTC clusters	3.5 ml min <sup>-1</sup>	4	Tested on pleural and abdominal effusions No	119
Single-looped spiral	Large particle	2023	FI	Inertial Size	Numerical simulation only	N/A	2	Cell staining	120
U-turn spiral	Large particle	2023	FI	Inertial Size	>90% of larger particles	1.7 ml min <sup>-1</sup>	2	Yes	121
Cascaded spiral	CTC	2023	FI + SI	Inertial + filtration	>85% for SGC-7901 cells, A549 cells and LoVo cells >90% in rabbit blood	300 µl min <sup>-1</sup>	2	Yes No	122
N/A	CTC	2014	EF	Size mMACS	Depends on antigen chosen and expression levels on cells of interest <~200 non target cells captured	2 to 40 ml h <sup>-1</sup>	3	No Cell staining Washing buffers	123
isoflux	CTC	EF	MACS					Fluxion bioscience	
Parsortix	CTC + CTC and clusters	2015 and 2018	SI	Filtration	54.4% PC, 57.3% DU145 and 54.7 to 78% MCF7 (study dependant) Purity of PC3 in blood is 4.6%	~5 ml h <sup>-1</sup>	2	Yes 1: 1 dilution 124, 125	126
Slanted spiral	CTC	2014	FI	Inertial Size + compressibility	80% T24, 85% MCF7, 87% MDA-MB-231 4 log WBC depletion 70% with SW480 cell lines 99.99% depletion of WBC	1.7 ml min <sup>-1</sup>	2	RBC lysis required.	127
CROSS chip	CTC	2019	SI	Size Filtration Size	80 µl min <sup>-1</sup> and <4 ml whole blood per chip (4 sections)	80 µl min <sup>-1</sup> and <4 ml whole blood per chip (4 sections)	2 No No No	127	

Table 2 (continued)

Device name	Target fraction	Year	Category	Mechanism and separation characteristic	Efficiency and purity	Sample speed or max volume	Chip complexity (1 is simple, 5 is complex)	Pre-processing and running buffers required	Reference
Celsee (now BioRad genesis)	CTC	2014 and 2016	SI	Filtration	81% MCF7 and 83% for MDA-MB-231	~1 ml min <sup>-1</sup>	4	Fixation prior followed by 2x dilution	128, 129
Vortex	CTC	2014	FI	Size Inertial	27% to 42% at 40× blood dilution	4 ml min <sup>-1</sup>	2	Washing buffers 20× dilution	130
Oncobean	CTC	2014	SI	Size Affinity capture EpCAM	Purity of 57–94%	1 to 10 ml h <sup>-1</sup>	2	Washing buffers	131
Cluster-chip	CTC clusters	2015	SI	Filtration	99% of MDA-MB-231 cluster >4 cells	2.5 ml h <sup>-1</sup>	3	No	132
NanoVelcro CTC chip	CTC	2013	SI	Shape Affinity capture EpCAM	—	0.5 ml h <sup>-1</sup>	3	Cell staining	133
ieSCI-chip	CTC	2022	FI + SI	Inertial + filtration	80–95% with cell lines	1.4 ml min <sup>-1</sup>	5-single cell immunoblotting included	Washing buffers RBC lysis and dilution	134
MyCTC	CTC and CTC clusters	2022	SI	Filtration	87 to 98.5% with cell lines 89% with MCF7 in isolated WBCs	50 µl min <sup>-1</sup>	5 as it allows drug testing on the same chip	No	135
DLD arrays for large and small cluster separation	CTC clusters	2017	SI	Size DLD	Large clusters ~98%, smaller clusters ~65% in whole blood.	Up to 1 ml hr <sup>-1</sup>	4	No Yes	136
N/A	CTC	2011	FI	Size and asymmetry Inertial Size	>5 log depletion of RBCs 10–43% of HeLa cells Not defined	7.5 × 10 <sup>6</sup> cells per s <sup>-1</sup>	2	No Yes Dilution to 1% haemocrit required	137
Herringbone-chip (HB-chip)	CTC	2010	SI	Affinity capture EpCAM	91.8% of PC3 cells at 1.2 ml h <sup>-1</sup> (large chip) >40%	1.5 to 2.5 ml h <sup>-1</sup> up to ~4 ml	2	No (buffer used to flush unbound cells post capture)	138
i-DLD sorter	CTC	2019	FI + SI	Inertial + DLD Size	14% purity in cell lines spiked into WBC	400 µl min <sup>-1</sup>	4	No	139
CTC-chip	CTC	2007	SI	Affinity capture	91.34% recovery in blood 17.68% purity in blood >60% in cell lines expressing variable levels of EpCAM	1 to 2 ml h <sup>-1</sup> (efficiency drops when >2.5 ml h <sup>-1</sup> )	2	No	140
Geometrically enhanced differential immunocapture (GEDI)	CTC	2010	SI	Affinity capture PSMA	Average purity was 49% in metastatic prostate cancer to 67% in colorectal cancer 85% of LNCAP cells in blood 62% purity	1 ml h <sup>-1</sup> up to 1 ml	2	No (buffer used to flush unbound cells post capture)	141



Table 2 (continued)

Device name	Target fraction	Year	Category	Mechanism and separation characteristic	Efficiency and purity	Sample speed or max volume	Chip complexity (1 is simple, 5 is complex)	Pre-processing and running buffers required	Reference
Graphene oxide (GO) chip	CTC	2013	SI	Affinity capture	>87% of MCF7 in whole blood when >10 cells spiked in	3 ml h <sup>-1</sup>	3	No	142
Hydroseq	Cells	2019	SI	EpCAM Filtration	Not defined ~70% of targets cells were successfully paired with a bead	N/A	>5	No Is used for scRNASeq and requires lots of prep	143
Acoustophoresis	Cells	2019	EF	Size Acoustophoresis	Not defined 60–97% recovery Purity is inversely related to purity in blood ~75% when tested for cMYC and EpCAM capture of PC3 cells in blood	100 µl min <sup>-1</sup> and 1 × 10 <sup>6</sup> cells per ml <sup>-1</sup>	5	No Sorting buffer required	144
N/A	Cells	2021	EF	Affinity capture	Not defined ~90% recovery with HeyA8, MDA-MB-231 and LNCap 83% depletion of WBC in CTC fraction	2 ml h <sup>-1</sup>	4	Fixation, permeabilization and cell staining	145
3d printed monolithic device	CTC	2019	SI	Epitope expression + Affinity capture + filtration	Not defined ~90% recovery with HeyA8, MDA-MB-231 and LNCap 83% depletion of WBC in CTC fraction	500 µl h <sup>-1</sup> per layer, thus a 32-layer device can run at 16 ml h <sup>-1</sup>	4	No Cell staining	146
Monolithic CTC-iChip	CTC	2017	EF + FI + SI	Epitope expression and size DLD + inertial + MACS	Median recovery of 99.5% across multiple cell lines 445 WBCs per mL of input blood	1 ml min <sup>-1</sup>	5	Wash buffer required Cell staining	147
Cascaded filter deterministic lateral displacement (CFD)	CTC	2021	SI	DLD	>96% for k562 and A549 cell lines	1 ml min <sup>-1</sup>	4	5 : 4 dilution (blood : PBS) Running buffer required	148
Non-equilibrium inertial separation Array-XL (NISA-XL)	CTC clusters	2020	SI + FI	Size Inertial + filtration	WBC removal of 99.995%, RBC depletion is 100%	Depends on application but >30 ml h <sup>-1</sup>	4	1 : 1 dilution No	149
Vortex HT	CTC	2016	FI	Size Inertial	80% final recovery 4.2 log <sub>10</sub> reduction in WBC	>30 ml h <sup>-1</sup>	3	10× dilution Running and wash buffer required	150
N/A	CTC	2009	SI	Filtration	Assume similar to original vortex	7 ml min <sup>-1</sup>	2	1 : 2 dilution	151
Fluid-assisted separation technology (FAST)	CTC	2017	EF + SI (LOD)	Size Filtration	~80% for MCF-7, MDA-MB231 and HT-29 cell lines	0.7 ml h <sup>-1</sup>	2	No None	152
All-in-one centrifugal microfluidic device for CTCs	CTC	2014	EF + SI (LOD)	Size Centrifugation + filtration	Purity >85% at 5 kPa >96% for MDA-MB-231, MDA-MB-436, AGS, MCF7 and HCC78	>3 ml min <sup>-1</sup>	5 but simple to run	PBS to wash None	153
Fully automated CTC isolation platform	CTC	2014	EF (LOD)	Size Centrifugation	>2.5 log depletion of WBC ~55% MCF7 in 1 ml blood	3 ml in 20 s for filtration	5 but simple to run	Microbeads added to blood No	154



Table 2 (continued)

Device name	Target fraction	Year	Category	Mechanism and separation characteristic	Efficiency and purity	Sample speed or max volume	Chip complexity (1 is simple, 5 is complex)	Pre-processing and running buffers required	Reference
Multi-flow straight channel	CTC	2019	FI	Inertial	>93% recovery for H640 and ~80% for HCC827	100 $\mu\text{l min}^{-1}$	2	RBC lysis + dilution in PBS	155
DFF cascaded spiral system	CTC	2013	FI	Size	>87% purity	3 ml $\text{h}^{-1}$	3	Running buffer	156
				Inertial	85% with cell lines			2 $\times$ dilution	
				Size	Purity of ~10% in clinical samples			Running buffer	

## Fluid interactions devices

Microfluidic devices that separate blood into its constituent elements using fluid interactions do so through a complex mix of physical forces that can be largely explained through fluid mechanics. Commonly, these devices rely on observed effects such as the Zweifach–Fung effect, the Fareheus effect forces, and forces such as the Dean drag force as well as inertial lift forces that are leveraged in inertial devices. This category includes devices that can separate plasma or CTCs. Plasma collection is predominantly achieved *via* use of the Zweifach–Fung effect and the Fareheus effect forces, while inertial devices are common in CTC enrichment and have been effectively used in cancer that produce CTCs that are larger than the majority of blood cells.

## External force/active microfluidics

Devices that use external forces are the most varied category and whilst forces such as electrophoresis, dielectrophoresis, acoustophoresis, and magnetophoresis are often employed, most devices can further be subdivided into one of two categories: 1) those reliant on labelling the targeted fraction with either a specific tag (often facilitated by protein-antibody interactions, or complementary DNA binding), and 2) those that operate in a label free manner. Except for acoustophoresis and lab-on-a-disk devices, devices in this category are generally focused solely on the isolation of CTCs and CTC clusters.

To help understand how microfluidic blood fractionation in cancer liquid biopsy has developed, a timeline of device development is shown in Fig. 2. For simplicity, the methods are separated into those that allow plasma fractionation and those that are focused on CTC and CTC cluster separation. Microfluidic devices for plasma fractionation are still relatively rare but those that allow CTC, and CTC cluster isolation have exploded since around 2014. The methods have been further colour coded according to whether they fall into the categories of solid interactions devices (red), fluid interactions devices (green) or external force/active devices (blue), those that utilise a combination of mechanisms are illustrated as black dots.

### 4.1. Solid interactions devices

Microfluidic methods relying on physical interactions include: 1) physical filtration, 2) deterministic lateral displacement (DLD) and 3) affinity surface capture. The simplified representation of the working principle of devices in this category is shown in Fig. 3 while specific examples of devices are shown in Fig. S1.†

**4.1.1. Physical filtration.** This category includes devices that either rely on small filter pore sizes to prevent the passage of cells into the cell-free collection channels or specifically designed cell capture geometries that can capture CTCs/CTC clusters based on their larger size and other physical properties such as deformability. As a result of the extremely small pore sizes required and the overwhelming

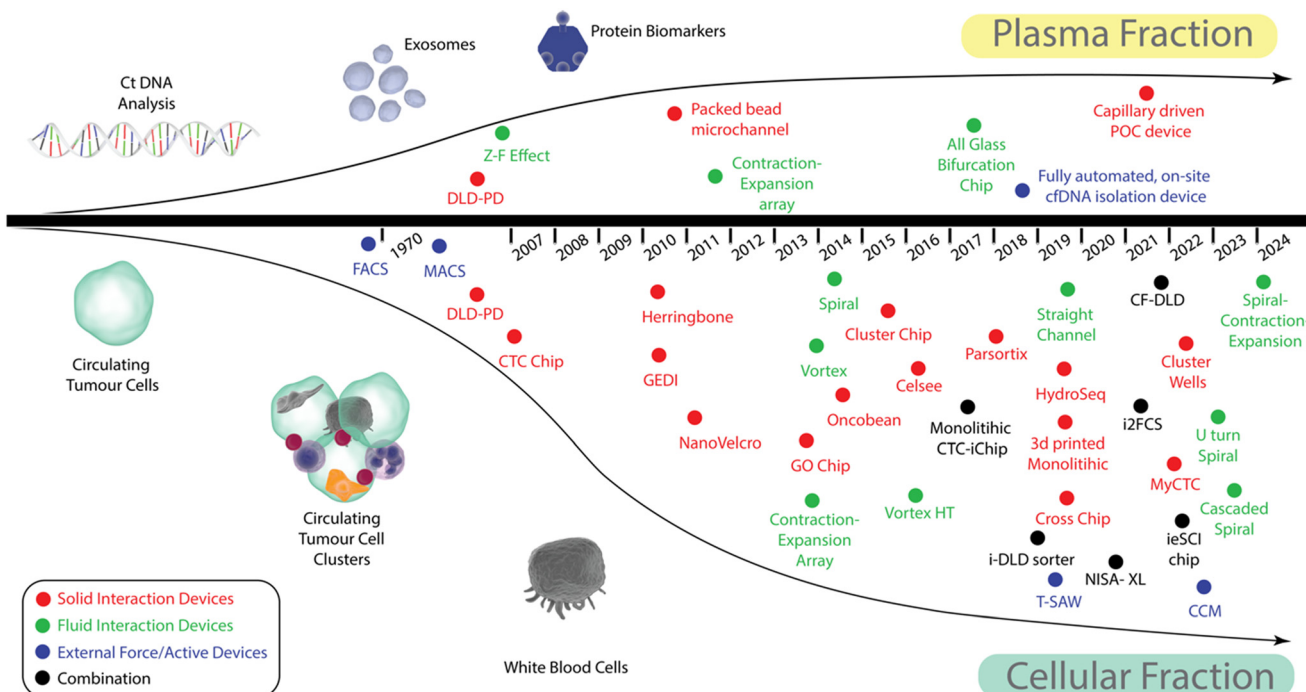


**Fig. 2** Timeline of tools for blood fractionation. To provide clarity, the timeline has been split to show those devices that can provide plasma or those predominantly concerned with cellular enrichment. Devices have further been colour coded according to whether they fall into the categories of solid interaction devices (red), fluid interaction devices (green) or external force/active devices (blue), those that utilise a combination of mechanisms are illustrated as black dots. Top: Shows the devices that have been used to fractionate plasma containing cfDNA from blood. Bottom: shows the devices that have been developed to allow cellular evidence of cancer to be detected in the peripheral blood draws. Devices in this category overwhelmingly focus on CTC enrichment.

number of RBCs that need to be filtered out, designs that aim to minimise clogging have been developed. This has been achieved with 1) carefully designed filter geometries, 2) larger channels that can be packed with beads (10  $\mu\text{m}$  to 20  $\mu\text{m}$  diameter) to create a filter bed with a greater filter surface area than achievable with individual channels created during the process of standard lithography<sup>106,115,158</sup> (Fig. S1A†), 3) devices that incorporate the use of commercially available filter membranes into devices with large surface areas,<sup>146,159</sup> 4) the use of cross flow filtration<sup>108,115</sup> (Fig. S1B†), 5) antibody mediated debulking of the sample prior to filtrations or separation,<sup>146,160</sup> and 6) incorporating a mechanism to provide and active clearing of the filter bed.<sup>108,161</sup> These approaches work as they either reduce the number of cells that the filters must prevent from passing (debulking), increase the available surface area (thus increasing the throughput possible before the filter becomes blocked) or actively clear the filter area (so that the device can run for a longer period before the filter is overwhelmed with particles blocking the passage of the plasma).

Devices that use physical filtration to extract plasma may produce plasma with high purities, but they tend to operate at very low flow rates and have a very low total blood processing volume. When low extraction volumes are coupled to the low concentrations of cfDNA found in the plasma (estimated at around 1000 genomes in 1 ml of blood plasma<sup>65</sup>), the sensitivity of the downstream assay can be

severely compromised. The maximum sensitivity can be calculated based on the average yields of cfDNA in plasma and the weight of the human genome to calculate the equivalent genomes present in the extracted cfDNA. To put this in perspective, as the diploid human cell contains approximately 6.5 pg. of DNA<sup>162</sup> and the human (haploid) genome would weigh half of this (approximately 3 pg), in systems such as those proposed by Shim *et al.*, that can only process 20  $\mu\text{l}$  of whole blood,<sup>106</sup> the extractable amount of cfDNA would be around 180 pg or 60 genomes (based on a haematocrit of 45% and an cfDNA yield of 20 ng  $\text{ml}^{-1}$  of plasma). Even assuming 100% cfDNA recovery and conversion of cfDNA into measurable product, assays relying on such low inputs are unlikely to contain sufficient starting ctDNA and would not be suitable for sensitive detection of cancer. This fact is further highlighted by systems such as those proposed by Szydzik *et al.* which only yield 180 nl of plasma.<sup>108</sup>

Filtration and solid capture approaches for CTCs and CTC cluster capture have also been created.<sup>132,146,151</sup> Due to the overwhelming numbers of RBCs, these are often implemented after RBC depletion. This depletion can be *via* osmotic RBC lysis, RBC depletion with MACS or *via* on-chip RBC depletion.<sup>115</sup> In some cases, depletion of white blood cells (usually *via* CD45 mediated immunogenic capture) is also performed.<sup>146</sup> This, however, would not be suitable for heterogenic CTC clusters containing CD45 positive immune



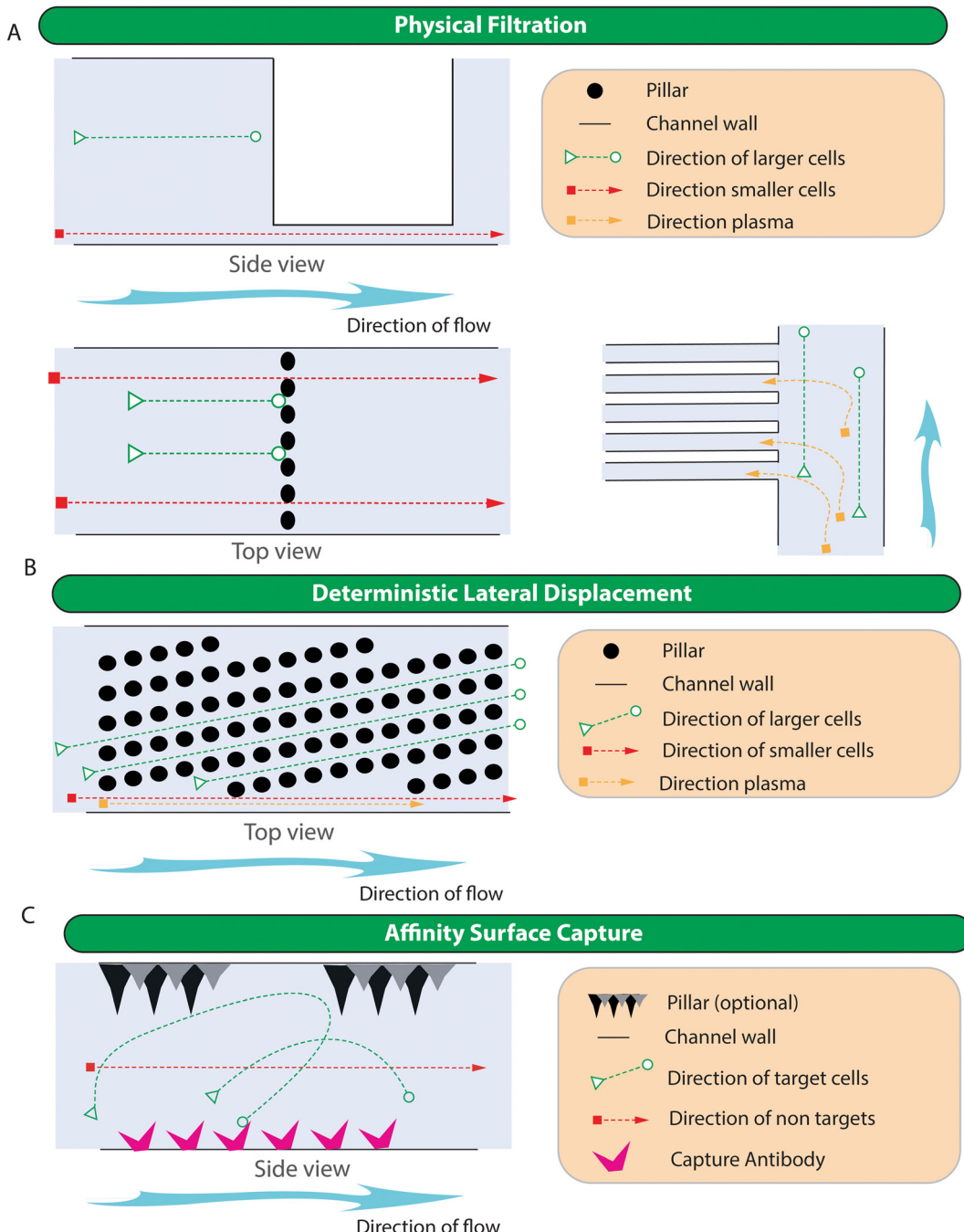


**Fig. 3** Schematic representation of the working principles for solid interaction microfluidic device in blood fractionation. A) Physical filtration devices use physical barriers to block the progress of cells; this can be used to block all cells entering plasma collection channels, to exclusively allow small cells such as RBCs to progress through into different parts of the chip (usually used for RBC depletion) or to capture larger CTCs in a particular region of the chip. B) Deterministic lateral displacement devices use offset pillar arrays to move cells above a defined critical diameter across the direction of flow and thus enable size-based separation. C) Affinity surface capture devices rely on the expression of cell surface proteins to enable exclusive capture of cells by tethering antibodies against specific proteins to the chip and bringing cells into contact with them. Once bound to these antibodies, the cells can no longer move in the direction of flow and are thus captured.

cells, as the clusters would likely be removed from further analysis. Filtration for CTC enrichment generally functions by retaining CTCs and letting the smaller cells through. In some cases, these use commercially available filters (*i.e.* 3D

printed Monolithic device<sup>146</sup>), in other cases, the filters are created as part of the device design. Examples of this include the Cross chip (Fig. S1E†) which creates a basic single row filter to prevent large cells from passing,<sup>127</sup> the Parsortix

system (Fig. S1D†) which uses a graduated step filter and tangential flow to prevent larger cells from passing into the waste stream,<sup>124,125</sup> and a device in which perforated cups, oriented so that the cup opening faces the direction of fluid flow, are designed in order to capture large CTCs while letting smaller cells to pass through.<sup>151</sup> CTC clusters can also be captured using physical filtration approaches. An example of such a device includes the Cluster-Chip which uses carefully arranged triangular pillars to capture multilobular CTC clusters. Clusters are held in place against the vertices of the triangular pillar using the pressure of the fluid flow to prevent the CTC cluster from being carried along the flow streams.<sup>132</sup>

**4.1.2. Deterministic lateral displacement.** Deterministic lateral displacement (DLD) devices take advantage of the fact that pillar/post arrays can be created to force cells above a certain size to move laterally in relation to the direction of fluid flow. DLD devices have extraordinary resolving capacity and are capable of separating particles with a resolution of as little as 10 nanometres.<sup>163</sup> The particle size at which this movement occurs is known as the critical diameter (dc) and can be calculated by the equation  $dc = 20\% \times 2w$  (where w is the separation gap between the pillars).<sup>83</sup> These devices are generally created using an array laid out in one of two ways. The first being the row shifted parallelogram array and the second being the rotated square. Work from Vernekar *et al.* has shown that the rotated-square arrays are less prone to anisotropic permeability and therefore provide more consistent performance.<sup>164</sup> Work to use DLD approaches to separate plasma from the blood has successfully resulted in the simultaneous separation of plasma and cells from undiluted blood<sup>102</sup> (Fig. S1C†). Although this multistage device did result in plasma separation with a claimed theoretical achievable efficiency of 100% with no contaminants above 1  $\mu\text{m}$  in diameter, the flow rate was only 0.4  $\mu\text{l}$  per minute. Systems such as this would therefore process only 24  $\mu\text{l}$  of blood each hour. Considering a cfDNA yield of 20 ng  $\text{ml}^{-1}$  of plasma, a haematocrit of 45% and perfect extraction of cfDNA this is equivalent to approximately one genome every 8 min.

Although not common, DLD devices can also be used to separate cells based on size. For example, the DLD-FD device designed by Davis *et al.* could separate cells based on a diameter above 9  $\mu\text{m}$ .<sup>102</sup> In this way, RBCs could be depleted from whole blood. Whilst these devices can provide extremely accurate size selection, they are almost always prohibitively slow for use in all but the lowest volume clinical assays. Traditional DLD devices are also prone to clogging<sup>149</sup> and thus may not yet be robust enough to be put into routine clinical workflows. Recently however, a modified pillar-post structure based around the concept of filtered deterministic lateral displacement has allowed rapid fractionation of CTCs through a two-step process involving the initial debulking of small cells, followed by a secondary fraction process aimed at purifying CTCs based on size.<sup>148</sup> The device uses a modified DLD pillar design in which a filter channel is incorporated

into the pillars themselves. This decreases the critical diameter when compared to pillar designs without the filter (*i.e.*, the filter DLD pillar design has an effective critical diameter of 10  $\mu\text{m}$  while a non-filtered equivalent DLD array would have a critical diameter of 15  $\mu\text{m}$ ). The first stage of the device allows parallel processing of the sample to remove RBCs. Following RBC depletion, the sample is combined with a flow buffer to enrich CTCs. This approach depletes 100% of RBCs and >99.95% of WBCs with a high capture rate for large CTCs and allows blood to be processed at fluid flow rates of 1  $\text{ml min}^{-1}$  and low fluid velocities ( $\sim 1.5 \text{ cm per s}^{-1}$  with only a 1:1 dilution of whole blood<sup>148</sup>) (Fig. S1K†).

CTC clusters can also be enriched using DLD. The NISA-XL device proposed by Edd *et al.* is reported to have on-chip CTC cluster yields of 100% at flow rates of more than 30  $\text{ml hour}^{-1}$  and can run with Haematocrit level of up to 20% (ref. 149) (Fig. S1J†). Additionally, Au *et al.* used an integrated 2 stage DLD array to enrich large and asymmetrical clusters from whole blood<sup>165</sup> (Fig. S1I†). They showed that, in whole blood, large clusters could be collected with an efficiency of around 98% while the smaller, asymmetrical clusters performed worse with an efficiency of just around 65%. Like many DLD devices, the device was relatively slow and could only run 500  $\mu\text{l}$  of blood per hour.

**4.1.3. Affinity surface capture.** Affinity surface capture devices directly tether the capture antibody to the substrate of the microfluidic chip. We have included affinity surface capture devices in the category of solid interaction devices as they rely on a cell/particle to come in contact with an antibody that is directly tethered to the device. Affinity-based microfluidics capture methods are perhaps the most common of all microfluidic-based CTC capture devices and include devices such as the Oncobean<sup>131</sup> (Fig. S1F†), Nanovelcro,<sup>133</sup> CTC chip,<sup>140</sup> GO Chip<sup>142</sup> (Fig. S1G†), GEDI,<sup>141</sup> and Herringbone-chip<sup>138</sup> (Fig. S1H†). Nagrath and colleagues proposed a microchannel, called “CTC-chip” for separation of CTCs from patient blood. In this channel, micro posts were functionalized with an anti-EpCAM antibody, providing specificity for capturing CTCs expressing this epithelial cell marker.<sup>140</sup> To increase the efficiency of capturing rare cells, the interaction between cells and the coated surface needs to be high. To achieve this, the “Herringbone-chip” was developed. It works by generating a vortex in the coated microchannel in order to increase the number of times a cell comes into contact with the chip surface. Despite the increased surface interactions, the recovery rate for prostate cancer cells in this channel was still only reported to be more than 21% using anti-EpCAM antibody.<sup>138</sup>

The effectiveness of affinity-based systems is dependent on a number of factors, including 1) the specificity of the antibody chosen, 2) the ability of the devices to bring the cell into contact with the capture antibody,<sup>133,138</sup> 3) the balance between the forces generated in the devices itself,<sup>140</sup> 4) the avidity of the antibody used (*i.e.* the total binding strength of the antibody to the cell), and 5) the antibody dissociation constant.<sup>166</sup> Affinity-based methods are suitable when a



particular epitope is exclusively expressed on the surface of CTCs (positive selection) or when it is known that the CTCs do not express a particular marker (depletion). Commonly CTCs have been targeted using EpCAM,<sup>44,140</sup> GD2,<sup>167,168</sup> EGFR,<sup>166,169</sup> PSMA,<sup>141</sup> HER2,<sup>170</sup> and HER3.<sup>169</sup>

Whilst diseases such as breast, colon, lung, and prostate cancer have utilised EpCAM mediated binding, it has been shown that by accounting for EpCAM negative CTCs, the number of patients in which CTCs can be found increases.<sup>21,171</sup> In other diseases that lack EpCAM expression, independent methods are required.<sup>172</sup> For example, markers such as GD2 in neuroblastoma and CD99 in Ewing's sarcoma, although expressed by cancer cells, are not restricted to CTCs alone<sup>167,173</sup> and therefore require technologies, such as flow or imaging cytometry, that can perform hierarchical classifications such that the CD99 positive population can be enriched for CTC by selecting only CD45 negative cells.<sup>173</sup> Additionally, many carcinomas will undergo an epithelial-to-mesenchymal transition (EMT) as part of the metastatic cascade. During EMT, the epithelial cell surface marker EpCAM is downregulated or lost,<sup>174</sup> and as a result, affinity-based methods relying on CTCs being separated using EpCAM will not be suitable.<sup>147,174-177</sup> Examples of the loss of EpCAM during cancer progression to metastatic disease have been shown in renal cell carcinoma,<sup>47</sup> breast cancer,<sup>178,179</sup> and particularly in CTC clusters rather than individual CTCs.<sup>12</sup> To bypass the requirement for CTCs to express a specific target molecule, affinity-based methods have been developed to deplete non-CTCs, these often target the immune cell marker CD45.<sup>146</sup> Whilst effective at removing WBC contamination, these approaches will also deplete CTCs that are travelling as clusters composed of immune cells.

While affinity based devices almost exclusively rely on cell surface expression of proteins, novel systems that allow separation based on intracellular proteins have also been developed;<sup>145</sup> however, this is far from a standard approach and requires cell fixation and permeabilization. Nonetheless, it provides an interesting and potentially beneficial approach in some cases. The system works by first fixing and permeabilizing the cell before staining with an antibody raised against an intracellular protein target. Following antibody binding, magnetic nanoparticles conjugated to an oligo that is complementary to a sequence on the antibody itself are introduced. The cells are then flown through a microfluidic chip with a progressively decreasing magnetic field to allow separation based on protein expression levels. This approach removes the need to restrict potential CTC markers to those expressed only on the cell surface and can be used to directly target therapeutic protein targets such as c-Myc.<sup>145</sup>

#### 4.2. Fluid interaction devices

Microfluidic methods relying on fluid interactions utilise the working mechanism of 1) plasma skimming and the Fareheus effect, 2) bifurcation effect, and 3) inertial focusing.

Plasma skimming and the Fareheus effect as well as the bifurcation effect are exclusively used for the collection of the plasma while inertial focusing, in all its forms, is predominantly used to purify cells based on size. The simplified representation of the working principle of devices in this category is shown in Fig. 4 while specific examples of devices are shown in Fig. S2†.

**4.2.1. Plasma skimming and the Fareheus effect.** The Fareheus effect describes the propensity of RBCs to position themselves in the centre of tubes with a diameter of less than 0.3  $\mu\text{m}$ .<sup>180</sup> The cell-free layer (CFL) is dependent on the diameter of the channel, the haematocrit, and flow rate.<sup>181,182</sup> Considering these factors, it is possible to design a device that essentially skims a small portion of the CFL while leaving the majority of cells untouched in the main channel.<sup>103,183</sup> As the relative CFL thickness becomes smaller as the tube diameter increases many of the devices relying on the Fareheus effect utilise small channels. Additionally, as the CFL thickness also decreases with increasing haematocrit dilution of whole blood is often performed. Modelling by Fedosov *et al.* showed that the thickness of the CFL in a 40  $\mu\text{m}$  diameter tube decreased from around 5  $\mu\text{m}$  when the haematocrit was 15% (diluted blood) to under 5  $\mu\text{m}$  when the haematocrit was 45% (normal blood).<sup>181</sup>

**4.2.2. Bifurcation effect.** The bifurcation or Zweifach-Fung effect can be observed as the tendency for cells flowing through a bifurcation to preferentially travel in the post bifurcation channel with the highest flow rate. Experimentally, devices relying on the Zweifach-Fung effect work best when the flow ratios between the channels exceed 1 to 6<sup>184</sup> and rising haematocrit levels result in smaller CFLs and poorer plasma purities.<sup>185</sup> Nonetheless when designed and implemented appropriately, plasma purities of >99.5% can be achieved, but yields are often poor 1–6%.<sup>104</sup> A number of device designs exist in this space; importantly, these devices have larger feature sizes than either physical filtration or plasma skimming devices and thus operate at significantly elevated flow rates.<sup>104,110,186,187</sup>

Collection of the plasma using plasma skimming or the bifurcation approach can result in high purity, but throughput tends to be very low, and yields can be poor. In devices such as those described by Kuan *et al.* and Yang *et al.* (Fig. S2A†) that operate at 0.3  $\text{ml min}^{-1}$ , 10  $\text{ml h}^{-1}$  respectively,<sup>115,184</sup> the volume of plasma processed would be insufficient as it would only yield between 90 and 162  $\text{pg}$  of cfDNA per hour. An exception to this may be the all glass bifurcation chip<sup>110</sup> that can operate at 700  $\mu\text{l min}^{-1}$  and return 74% of the plasma with only a two (2) fold dilution of the blood (Fig. S2B†) and a PDMS chip by Tripathi *et al.* that can operate at 500  $\mu\text{l min}^{-1}$ .<sup>104</sup>

**4.2.3. Inertial focusing.** Inertial microfluidics is used to focus a particle into a particular region of a microfluidic channel. In a straight channel, particles and cells are affected by inertial lift forces that include shear-induced and wall-induced lift forces. The balance of these two forces creates equilibrium positions where particles will tend to sit.<sup>188</sup> The



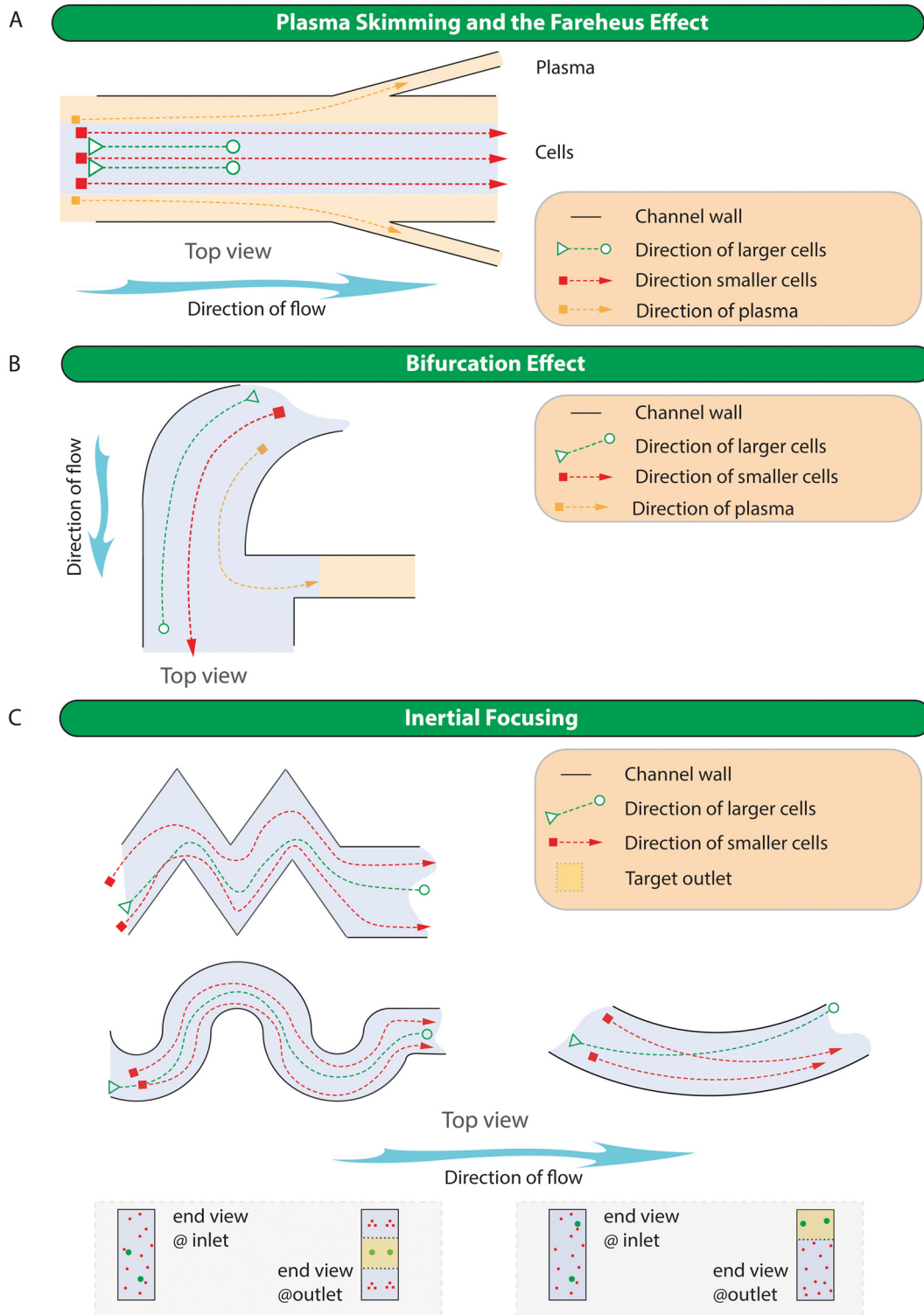


**Fig. 4** Schematic representation of the working principles for fluid interaction microfluidic devices in blood fractionation. A) Plasma skimming and the Fareheus effect devices. The Fareheus effect occurs as cells tend to orient themselves toward the centre of the channel and can be used to collect plasma from the cell free region that exist close to the walls of small vessels B) bifurcation effect devices. The bifurcation effect occurs as cells tend to migrate towards faster flowing fluid streams after they encounter a bifurcation or split, C) inertial focusing devices come in many different configurations including spiral, serpentine, straight, and contraction expansion devices, whilst the physics in these devices are different, they all work by allowing target cells to be trapped in equilibrium locations within the fluid flow. These devices are often used for CTC enrichment but have also been applied to plasma separation.



location and the number of equilibrium positions are governed by the channel shape and its hydrodynamic diameter.<sup>189</sup> In the case of non-straight channels such as spiral, serpentine, or contraction-expansion microchannels, Dean drag forces also contributed to the focusing particles within the channel cross-section. For a given channel design, the value and strength of inertial lift and Dean drag forces are related to the particle size.<sup>190</sup> Within the inertial regime, particles above a certain threshold in PDMS-made channels ( $a_p/h > 0.07$ , where  $a_p$  is particle diameter and  $h$  is channel height) are heavily influenced by inertial forces; hence, one can accurately focus cells into lateral position within the channel.<sup>191</sup> This criteria has been refined for rigid channels to be  $a_p/h > 0.04$ .<sup>192</sup>

In 2007 Seo *et al.* used a double spiral design to enrich 10  $\mu\text{m}$  particles by 660 fold<sup>193</sup> (Fig. S2D†). Inertial focusing channels have proven to be an extremely popular method to fractionate cells and particles from fluids. As such, in addition to single spiral devices with rectangular channel cross-sections<sup>194</sup> (Fig. S2E†), a number of spiral device variants have been created; these include cascaded spiral microchannels,<sup>156,195,196</sup> labyrinth-shaped channel<sup>197,198</sup> (Fig. S2F†), multiplexed spiral channels,<sup>199</sup> double spiral microchannel,<sup>200</sup> spiral with slanted walls,<sup>126</sup> triple parallelizing spiral device,<sup>201</sup> ordered micro-obstacles spiral device,<sup>202</sup> sequentially connected spiral channels,<sup>203</sup> single loop spirals,<sup>120</sup> and spirals that include u-turns.<sup>121</sup> Recently Zhu *et al.* developed a spiral device that incorporates contraction-expansion arrays in the last loop resulting in improved separation of both CTCs and CTC clusters at high flow rates (3.5  $\text{ml min}^{-1}$ )<sup>119</sup> (Fig. S2G†). Recognising the usefulness of the spiral design but acknowledging the need to further purify and isolate CTCs, Lu *et al.* designed a cascaded microfluidic chip consisting of an initial five loop spiral microchannel followed by an array of perforated cups to catch CTCs and to allow residual smaller cells to pass through to waste.<sup>122</sup> Furthermore, when Xiang *et al.* coupled a DLD array downstream of a spiral device, they showed improvements to capture purities and separation efficiencies.<sup>139</sup> Additionally non-spiral geometries for CTC enrichment include straight channels<sup>155</sup> (Fig. S2H†) and the contraction-expansion array (CEA) microchannel devices developed by Hur *et al.*,<sup>137</sup> Sollier *et al.*,<sup>130</sup> (Fig. S2I†), and Lee *et al.*<sup>204</sup> have been developed. These concentration-expansion arrays trap cells based on size in laminar vortices created in the areas of expansion.<sup>137</sup>

For CTC enrichment, inertial focusing has been applied to several cancers including breast,<sup>205</sup> prostate,<sup>206</sup> lung,<sup>207</sup> head and neck,<sup>157</sup> and glioblastoma.<sup>73</sup> These studies rely on the assumption that CTCs are larger than the majority of cells in the blood ( $>\sim 15 \mu\text{m}$ ); as such, the devices may have limited use in the capture of small CTCs. The inability to isolate small CTCs may be problematic as CTC heterogeneity suggests CTC sizes may vary, not only between cancers but within patients<sup>208</sup> and by the compartment in which they are found (*i.e.*, CSF CTCs *vs* blood CTC's).<sup>209</sup> A study by Mendear

*et al.* which assessed the size of CTCs (as captured by the cell search system – EpCAM capture and verified by Cytokeratin positive staining), showed that CTC size can vary significantly between tumour types and the compartment in which CTCs were found. For example, CTCs from colorectal and bladder cancer (7.5 and 8.6  $\mu\text{m}$  median diameters respectively) were much smaller than the cut-offs commonly used in the design of size-based CTC capture devices and importantly from lymphocytes (9.4  $\mu\text{m}$  median diameter), while CTCs isolated from breast cancer and prostate cancer, although bigger (12.4 and 10.3  $\mu\text{m}$  median diameters respectively) were not as big as generally assumed, and the breast cancer CTCs from the blood were significantly smaller than those found in the CSF (120.4  $\mu\text{m}^2$  *vs.* 141.3  $\mu\text{m}^2$  respectively). Furthermore, they showed that the cell lines often used to validate devices do not necessarily reflect the size of the CTCs found in the patient *e.g.* the average size for breast cancer CTCs in the blood (12.4  $\mu\text{m}$  median diameter) was significantly smaller than that of common breast cancer cell lines such as MCF-7 (18.4  $\mu\text{m}$  median diameter), T47D (18.35  $\mu\text{m}$  median diameter, and SKBR3 (22.01  $\mu\text{m}$  median diameter).<sup>209</sup> This finding is also supported in prostate cancer.<sup>208</sup> To overcome the issue of size-based heterogeneity, improve throughputs, and reduce contamination, Liu *et al.* have combined inertial focusing (serpentine channels) with MACs.<sup>116</sup> The device still requires RBC lysis and cell staining but achieves a flow rate of 60  $\text{ml h}^{-1}$  and reduces WBC contamination down to 507 WBCs per ml.

Inertial focusing has also been used for plasma separation;<sup>107,199</sup> however, this requires significant sample dilution, making the plasma unusable for many biological assays. By way of illustration, a standard blood collection tube used in adults has a maximum volume of 10 ml and commonly  $\sim 8$  ml is collected. If blood was to be fractionated in its undiluted state, the resulting fractions would be roughly 4 ml plasma and 4 ml cells (including RBCs). This volume is compatible with current extraction methods for cfDNA. However, if the blood was diluted even 1:10 such as described by Lee *et al.*,<sup>107</sup> then the resulting “plasma” fraction would have a volume of 40 ml and new cfDNA extraction methods would need to be devised. Furthermore, as described, the device only has a 60% RBC rejection rate and a 62% plasma yield (Fig. S2C†). If diluted to 1:100, so as to achieve a blood haematocrit of  $\sim 0.5\%$ ,<sup>199</sup> then the volume of plasma from which cfDNA is to be extracted would be 400 ml, thus extraction of cfDNA from diluted whole blood would be impractical and costly.

#### 4.3. External force/active microfluidics

Although more complicated than the passive approaches, active devices are more amenable to end-user modification. This is because, once created, devices that rely on fluid or solid interactions tend to have their parameters set during the device fabrication, while those that provide external forces can be tweaked according to the end user's preference.



For example, to select a new target cell in mMACS and mFACS, one simply needs to label cells with a new antibody, or if separation is achieved using acoustophoresis, it is possible to tune the applied field to separate particles with different characteristics including size and cell viability.<sup>210</sup> Devices in this category rely on the working mechanisms of 1) lab-on-a-disk, 2) acoustophoresis, 3) microfluidic magnetic associated cell separation (mMACS), 4) microfluidic fluorescent cell sorting (mFACS), 5) piezoelectric-membrane actuated mFACS, and 6) electrokinetic actuated mFACS. The simplified representation of the working principle of devices in this category is shown in Fig. 5 while specific examples of devices are shown in Fig. S3.†

**4.3.1. Lab-on-a-disk.** Centrifugal microfluidic platforms, often referred to as lab-on-a-disk systems due to their disc-like design, have emerged as promising tools for liquid biopsy and blood fractionation. These platforms leverage the principles of centrifugal force to manipulate fluid samples within microscale channels built onto a spinning disc. The rotation of the disc enables precise control over sample handling, mixing, separation, and analysis, all within a compact and portable format.<sup>211</sup>

Centrifugal microfluidics has been used for plasma separation. In 2006, Haeberle *et al.* presented a centrifugal microfluidic platform to isolate plasma from whole blood using a decanting structure. The device has been successfully utilized to extract 2 µl of plasma from 5 µl of whole blood, with a residual cell concentration of below 0.11%.<sup>212</sup> As another example, through the use of a curving channel with one-fourth of a turn, plasma of a blood sample with 6% haematocrit concentration can be isolated with 96% efficiency and achieved within 5–6 seconds.<sup>213</sup> The practicality of the devices was illustrated by performing prothrombin test<sup>213</sup> and creatinine test.<sup>214</sup> However, these volumes are a long way from being useable in modern liquid biopsy for genomic analysis and the need to dilute blood to known haematocrit concentrations is counterproductive for high-sensitivity assays where the number of targets into the system matters.

In 2022, Shing and colleagues presented a portable centrifugal microfluidic device for plasma separation. This device comprises multiple chambers and microchannels, wherein a plasma reservoir and a cell reservoir are interconnected and aligned with the centre of the disc. This configuration achieves a plasma purity of 99.9%, separation efficiency of 99.9% (with a blood haematocrit of 48%), and a plasma recovery rate of 32.5% within 50 seconds.<sup>215</sup> In another study, Lenz *et al.* introduced a microfluidic device designed for centrifugal serum separation from blood, suitable for on-site use. This system accommodates both hydrophilic and hydrophobic biomarkers. The cross-flow filtration mechanism efficiently separates serum from blood, comparable to conventional techniques, while preserving amphiphilic biomarkers within the serum for subsequent detection.<sup>216</sup> Hatami developed a fully automatic centrifugal microfluidic platform to isolate plasma for the isolation of

cell-free foetal DNAs (cffDNAs). Besides plasma separation, all the required steps for cfDNA extraction, including adding proteinase K, lysis buffer, binding buffer, washing buffer, and elution buffer, have been considered. To accomplish this goal, magnetic particles were utilized first to attach the cfDNAs, and then transfer them between the chambers.<sup>217</sup>

Centrifugal microfluidics has also been developed to advance CTC isolation from blood. For instance, Park *et al.* developed a centrifugal microfluidic platform aiming for fully automated, high-purity isolation of CTCs. Their approach utilizes a disc device with a triangular obstacle structure in the blood chamber to manipulate blood cells. CTCs are selectively bound to microbeads coated with anti-EpCAM, allowing for density-based isolation under a density gradient medium layer. The system can process 5 mL of blood, yielding isolated cancer cells within 78 minutes with minimal contamination of approximately 12 leukocytes per millilitre.<sup>154</sup> In 2021, two centrifugal microfluidic devices were developed for isolating rare cancer cells: a passive plan and a hybrid plan. The passive plan employs a contraction-expansion array (CEA) microchannel connected to a bifurcation region, while the hybrid plan uses a CEA microchannel reinforced with magnets to capture magnetically labelled target cells. Both designs were optimized and tested for isolating MCF-7 breast cancer cells from mouse fibroblast cells. The hybrid design, utilizing magnetite nanoparticles and permanent magnets, demonstrated superior performance (85% recovery rate at 1200 rpm) compared to the passive design (76% recovery rate at 2100 rpm). However, the passive design offers advantages such as simplified processing, compact size, and cost-effectiveness.<sup>218</sup> In a most recent study, a simple label-free centrifugal microfluidic device was proposed to separate cancer cells from whole blood samples using synergistic hydrodynamic effects, including Y-shaped microchannel, a contraction-expansion array (CEA) microchannel, and a bifurcation region. Experimental results demonstrated the successful separation of K562 cancer cells from diluted blood samples (ratio 1:1.2 × 105), achieving a high efficiency of 90% at an angular velocity of 2000 rpm<sup>219</sup> (Fig. S3E†).

Although centrifugal microfluidics removes the need for setting up complex pumps and collection systems, some challenges still require careful attention. Clogging is one of the major challenges within these platforms, although implementing filtration techniques can alleviate this challenge. Additionally, scalability and throughput are areas of concern due to the limited capacity for sample processing within these platforms.

**4.3.2. Acoustophoresis.** Acoustophoresis is a gentle, non-contact method whereby cells in suspension exposed to an acoustic standing wave field are affected by an acoustic radiation force.<sup>220–223</sup> A cell experiencing this force will move toward nodes or antinodes, and its movement depends upon physical properties such as density, compressibility, and size.<sup>224–227</sup> The implementation of acoustophoresis in microfluidic devices has gained significant appeal because it



## External Force/ Active Microfluidics

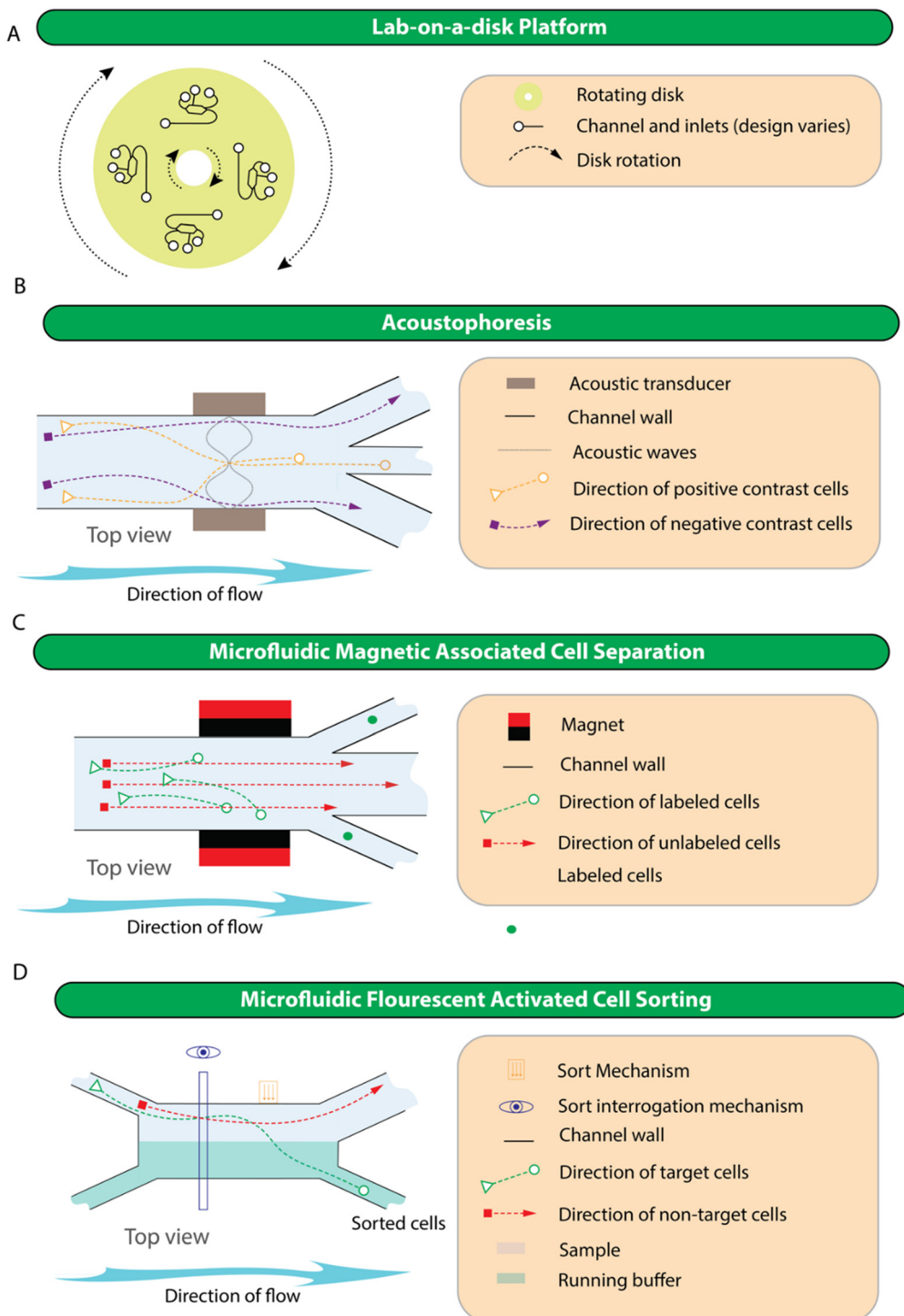


**Fig. 5** Schematic representation of the working principles for external force/active microfluidic device in blood fractionation. A) Lab-on-a-disk devices. Devices in this category can be designed for both plasma and CTC enrichment and whilst highly varied, all use rotational forces to help process the blood. B) Acoustophoresis can be used to separate blood into plasma and enrich for specific cell types. The example device shown uses a standing wave to focus cells at the node and the antinode depending on a cell's acoustic properties and the characteristics of the acoustic wave. Other devices can tune the wave to focus all cells so that plasma can be obtained. Acoustic waves can also be used as the sort mechanism in microfluidic cell sorting. C) Microfluidic magnetic associated cell separation. These devices require cells to be labelled with an antibody attached to a ferrous particle so that when the labelled cells enter a magnetic field they are deflected according to the polarity of the magnetic field. D) Microfluidic fluorescent activated cell sorting devices allow the interrogation of fluorescently labelled cells using a light source and detector(s) to enable active selection of cells based on expression or absence of certain markers. Fluorescent labels are often attached to antibodies, but this does not need to be the case and theoretically any fluorescent tag(s) can be used. Sorting the cell of interest can be achieved in a number of ways, these include piezoelectric-membrane actuated mFACS, acoustic wave actuated mFACS and electrokinetics.



is a miniaturised, label-free active separation approach that addresses the challenge of isolating rare cells within a heterogeneous population.<sup>221,228</sup> Microfluidic acoustophoresis systems are typically designed to separate particles or cells of different sizes or mechanical properties.<sup>221,225,226,229</sup> These systems have been applied to blood samples to separate the blood components in a continuous and biocompatible manner. Petersson *et al.* demonstrated the ability to perform plasma exchange of blood using a type of acoustophoresis known as bulk acoustic wave (BAW)-based separation.<sup>230</sup> Acoustophoresis has also been shown to isolate plasma from blood<sup>105</sup> (Fig. S3B†) and has the ability to isolate exosomes or other types of extracellular vesicles directly from whole-blood samples.<sup>231,232</sup>

In addition to plasma separation, acoustophoresis has also been demonstrated to remove platelets from peripheral blood progenitor cell products (PBPC and whole blood samples)<sup>233–235</sup> and to isolate circulating tumour cells (CTCs) from lysed or pre-treated whole blood.<sup>144,228,231,236–238</sup> Furthermore, acoustophoresis is also biocompatible, showing that cell viability was maintained during the separation process.<sup>228</sup> Olm *et al.* used electrophoresis to separate neuroblastoma cells (SH-SY5Y) from blood cells using a two-stage approach incorporated onto a single chip. The first stage was used to align all cells into 2 parallel bands so that they are appropriately oriented for the second stage with involved acoustically focusing the larger SH-SY5Y cell to the centre of the channel where they could be collected (Fig. S3G†). Using this device, they showed that they could recover between 60 and 90% of spiked in neuroblastoma cells.<sup>144</sup>

With time, acoustophoresis-based separation offers a pathway to enhance liquid biopsy applications and impact the field of translational medicine. However, it still suffers from poor yields and is yet to be convincingly applied to high volume plasma separation or to CTC isolation across a range of cancers.

**4.3.3. Microfluidic magnetic associated cell separation (μMACS).** Affinity-based capture methods rely on the cells of interest expressing an epitope for which an antibody can be raised. For CTC capture, these systems have tended to rely on cancer cells expressing the epithelial cell marker EpcAM. The only FDA approved system for CTC capture and enumeration, CellSearch, captures CTCs using a magnetic core nanoparticle conjugated to an anti-EpCAM antibody. There are many microfluidic-based MACS systems available for the detection of CTC. The cell search and the isoflux systems are perhaps the best known of these but there are others. However, the increasing recognition that EMT plays a significant role in many solid tumours means that these systems are likely to miss many of the CTCs that have undergone transition to a more malignant phenotype. Furthermore, whilst these and other mMACS systems can be modified to capture cells with alternate markers, they still overwhelmingly rely on a single cell surface target molecule.

Thus, they are likely to be missing the expected heterogeneity in the CTC population.

One way around the reliance on a single target for enrichment is to utilise a depletion approach. Microfluidic devices such as LPCTC-iChip platform<sup>239</sup> or the the monolithic CTC incorporate a combination of solid interactions (DLD array), fluid interactions (serpentine inertial focusing), and external forces (MACS) to achieve CTC enrichment<sup>147</sup> (Fig. S3D†). In the monolithic device, blood is firstly depleted of red blood cells and platelets *via* a DLD array before the nucleated cells (CTCs and WBCs) are focused using an inertial approach to allow labelled (CD45 positive cells) to be removed by two passes through a magnetic field. The first pass depletes WBCs with >6 MACS beads (targeting CD45, CD16, or CD66b) attached while the second pass cleans up those cells with more than one magnetic bead. Once WBC depletion is complete, CTCs are collected and concentrated for downstream validation.

**4.3.4. Microfluidic cell sorting (μFACS).** Identifying and isolating cells of interest from complex, heterogeneous mixtures in a sequential and rapid manner represents an essential process for many areas in clinical medicine. Microfluidic-based fluorescent activated cell sorting (μFACS) relies on fluorescent probes or stains to identify cells by type. The fluorescently labelled cells are flowed through a microchannel and encounter a focused laser that scatters into a photodetector. The fluorescent signal is then analyzed, and depending on the detection criteria, an external force is generated to displace the cell into a separate channel. This technique eliminates the production of aerosols and can support small sample volumes that are orders of magnitude smaller than conventional jet-in-air cell sorters. More importantly, μFACS can provide a means toward the isolation of rare target cell populations, such as the enrichment of circulating tumour cells (CTCs).

Several cell-sorting mechanisms have been used in microfluidic devices, including 1) piezoelectric actuation, 2) surface acoustic waves (SAW), and 3) pulsed laser-activated cell sorting (PLACS).<sup>240–242</sup> Piezoelectric-membrane actuation is a mechanism used in microfluidics whereby a piezoelectric element causes the deformation of a membrane adjacent to a microchannel to displace a particle of interest into a separate channel, usually in response to fluorescent detection.<sup>240,243–245</sup> This technique can sort individual cells at rates of up to several kHz per channel and can be easily parallelised for increased throughput.<sup>240</sup> The use of a piezoelectric actuator has been demonstrated to work in glass microfluidic chips, which is a more commercial and clinical friendly material when compared to the commonly used PDMS.<sup>240,244</sup> Acoustic waves have gained significant use in μFACS due to their ability to gently organize and/or displace cells or droplets into separate channels at fast rates.<sup>228,242,246–248</sup> Traditionally, this mechanism was used for applications where cells were not labelled. However, when combined with a fluorescent detection system, this mechanism can achieve switching times as short as 25 μs (ref. 242) (Fig. S3F†).



Electrokinetic mechanisms for fluorescent label-based microfluidic cell sorting are divided into three categories: 1) electrophoresis, 2) dielectrophoresis (DEP), and 3) electroosmotic flow.<sup>249</sup> Electrophoresis refers to the movement of particles in a uniform electric field due to their surface charge.<sup>249,250</sup> This mechanism takes advantage of the slightly negative charge most cells possess.<sup>251</sup> In contrast to electrophoresis, where cells move in a uniform electric field, DEP refers to the movement of cells in a non-uniform electric field due to their polarizability.<sup>249</sup> For movement in response to a dielectrophoretic force, cells do not need to possess a surface charge because, unlike a DC field, an alternating current (AC) can induce a dipole moment across the cell.<sup>249,250</sup> DEP is commonly used in droplet-based microfluidic applications, whereby cells are encapsulated into picolitre volumes for single-cell assays.<sup>252,253</sup> The use of DEP in a fluorescence-activated droplet sorter has been demonstrated to sort up to several or more thousand cells per second.<sup>254,255</sup> This technique also enables the compartmentalisation of cells into emulsions with antibody-coated beads to analyse the secretion of antibodies from cells for downstream sorting.<sup>256</sup>

Electroosmotic flow, on the other hand, moves the bulk fluid surrounding a cell due to the electrically induced migration of solvated ions.<sup>257,258</sup> This method, however, can generate bubbles and harmful compounds such as hydrogen peroxide, which can adversely affect cells.<sup>259</sup>

In addition to using electrokinetic forces in microfluidic FACS, it is also possible to harness this force for separation of plasma. As described in the filtration section, DEP is also used to clear filter beds during plasma fractionation<sup>108,161</sup> (Fig. S3A†). Xing *et al.* has also applied electrokinetics in the separation of plasma<sup>109</sup> (Fig. S3C†). However, whilst the system provided good plasma protein yields, the need to dilute blood to 4% haematocrit, the use of a high conductivity buffer, and the low processing volumes make the system not suitable for use in ctDNA based liquid biopsy.

## 5. Strengths and limitations of current microfluidic approaches

Traditional bulk separation methods of centrifugation and filtration have served as the foundation upon which liquid

**Table 3** Strengths of current microfluidic tools for plasma (ctDNA) and CTC analysis. It should be noted that not all the strengths are applicable to all devices

Plasma devices	
Strengths	Impact
Ability to handle low sample volumes	It can be very difficult to handle low sample volumes using conventional methods such as centrifugation. Microfluidic devices often have extremely low dead volumes and are therefore ideally suited for handling low input samples. Due to biological considerations, low input volumes often make ctDNA and CTCs analysis difficult; however, emerging techniques in high throughput proteomics and improved efficiencies in genomic preparations are reducing the volume of sample required
CTC devices	
Strengths	Impact
Many devices can process cell in parallel	Unlike techniques such as fluorescent activated cell sorting or flow cytometry, many microfluidic approaches for CTC enrichment allow parallel processing of individual cells. This can significantly increase the throughput and reduce the operational time for CTC enrichment. Shorter processing times may minimise pre-analytical variables and thus allow a truer reflection of biology
Many devices are label free	Techniques, particularly those that use fluid interaction and to a lesser extent external forces to separate CTCs, do not require prior knowledge of cell surface proteins on the CTC. This is useful when no markers are known or when biological process may be down regulating known cell surface markers
General	
Semi-automated nature of microfluidics	As many devices are semi-automated, the ability of an operator to affect outcomes can be minimised. This of course depends heavily on the device design so care should be taken here
Some devices have been specially designed to reduce the stress on cells during the fractionation process	Microfluidics can be designed to have low pressures and to minimise shear forces acting on cells. This means that the samples may be less affected by preanalytical factors that may otherwise lead to compromised results. This is device dependant and should be a consideration when assessing any device
Microfluidic devices generally have a small footprint and a low initial cost	Microfluidic devices are often relatively simple channels made from cheap material (active devices can be an exception to this rule). This makes the startup cost relatively low. They also tend to have small footprints meaning that they do not require a lot of laboratory space
Systems are generally closed and do not produce aerosols	Handling of primary samples can produce a biohazard for operators. The closed nature of many microfluidic devices increase operator safety of sample are not aerosolized and therefore more readily contained



biopsy has begun to offer crucial insights into cancer, while current microfluidic devices have, to some extent, filled the need for rapid processing of samples and the ability to effectively process low sample volumes. Current microfluidic tools have allowed numerous studies across a number of different cancers and have been instrumental in proving that liquid biopsy can provide a powerful mechanism to quantitatively assess tumour burden, measure metastatic potential through CTC enumeration and to track genomic changes as part of disease progression or in response to treatment induced change. Importantly, by enabling this on peripheral blood samples, liquid biopsy reduces the need for invasive procedures and can help improve the quality of life for patients during their cancer journey. To understand how microfluidics is contributing to enabling liquid biopsy, an overview of the general strengths of microfluidic approaches to blood fractionation is given in Table 3.

Despite the important role of bulk fractionation and current microfluidic methods in the development of liquid biopsy for cancer patients, there remains a critical need to further improve the processing of blood samples. This

process would ideally occur close to the point-of-draw and enable rapid sample processing and produce fractions that are suitable for multiomic liquid biopsy. There are, however, no solutions that allow a full multiomic workflow leveraging both ctDNA and CTC analysis at the same time. Furthermore, the current generation of microfluidic fractionation devices all have limitations that mean they are still not optimally suited to use in emerging next generation analysis pipelines. These limitations are shown in Table 4.

Despite the strengths of many microfluidic devices for blood fractionation in cancer liquid biopsy, the limitations shown in Table 4 suggests that there is now a need for new devices and a significant opportunity to improve on current microfluidics approaches for blood fraction in relation to cancer liquid biopsy. For example, a rapid, low-cost, point-of-draw fractionation method that allows the separation of all biologically relevant blood fractions into their constituent elements in a format compatible with multiple emerging downstream assays would be a game-changer. Such a device would allow each blood component to be safely stored under the correct conditions for downstream analysis without

**Table 4** Limitations of current generation of microfluidic tools for plasma (ctDNA) and CTC analysis. It should be noted that not all the limitations listed are applicable to all devices

Plasma devices	
Limitations	Impact
Speed of processing	To extract sufficient material (and hence equivalent genomes) for high sensitivity detection of cancer a significant amount of blood needs to be processed $>2$ ml. Some devices run at less than 1 $\mu$ l per minute, therefore retrieving enough cfDNA to perform the assays is impossible
Prone to clogging	Clogging of chips can prematurely terminate the collection of plasma and therefore reduce the overall yield of plasma from a run. The inability to collect all the sample prior to mechanical failure due to clogging has the effect of reducing yield and may compromise the purity of the sample
Often require dilution	Dilution of blood (sometimes by up to 100-fold), means that vast quantities of plasma will be collected. Even if this plasma was free from impurities and the yield was high, the volumes would prevent any meaningful downstream analysis and purification of cfDNA would be extremely difficult and likely cost prohibitive
CTC devices	
Limitations	Impact
Many cannot process whole blood and require dilution of RBC lysis	Blood dilution for CTC increases the processing time and whilst the effect is not as pronounced as with cfDNA (CTCs can be more readily concentrated) it nonetheless still provides potential delay to analysis. Where RBC lysis is utilised, CTCs are subject to unfavourable conditions and therefore subjected to unnecessary stress (which may result in experimentally induced changes)
Immunoaffinity methods require prior knowledge of protein targets	Whilst some cancers such as prostate, breast, lung, and neuroblastoma shed CTCs that express well-known cell surface markers, others do not have well-defined cell surface markers. In addition, most immunoaffinity methods rely on a single marker and given the well-known heterogeneity in CTCs (as a result of EMT) many CTCs may not be captured and the population is biased towards a single CTC subtype
There is no way to perform intracellular immunoaffinity collection in live cells	Whilst cell surface targets allow CTC enrichment in some cancers, many cancer specific epitopes are intracellular. Therefore, by relying on cell surface protein markers for live CTC enrichment, we are reducing the number of targets available. Furthermore, restricting to protein epitopes may be limiting, as cancer is primarily a disease of genetic alteration
Immunoaffinity depletion methods remove all cells that express the target	Methods that rely on depletion using an antibody/antibodies risk losing CTCs that either co-express the marker or are traveling as clusters that contain cells expressing the marker. Therefore, these methods will bias CTC selection, reduce capture numbers and may be blinded to the contribution of heterotypic CTC clusters
Size based methods assume all CTCs are above a certain size	Heterogeneity in CTCs size has been shown in several cancers. Therefore, the assumption that CTCs are always bigger than other cells in the blood means that smaller CTCs are lost



compromising the other biologically relevant fractions found within the blood and could simplify pre-analytical workflows.

## 6. Conclusion and perspectives

Liquid biopsy holds enormous promise in the clinical management of patients with cancer. Through longitudinal, high-sensitivity liquid biopsy, it is possible to detect disease early, track disease burden, monitor response to treatment, and understand disease heterogeneity. However, the ability to perform multiple assays from the one blood draw is still limited. As such, there remains an opportunity for a device that can rapidly isolate plasma and cells from low volume blood draws at the point-of-draw and to use microfluidics to change patient management and provide an important tool for the delivery of better patient outcomes.

By developing new devices that take the most effective parts of existing devices and combining these to simultaneously produce plasma and cellular fractions, it would be possible to provide plasma and cellular fractions compatible with emerging next generation approaches. For example, using a high efficiency system capable of separating cells and plasma at the point-of-draw would allow plasma,

cleaned from containing any residual cells, to be safely snap-frozen whilst CTCs and CTC clusters could be collected without the need to use troublesome preservatives that interfere with downstream RNA and cytometric profiling. This would also allow analysis of both ctDNA and CTC from a single blood draw, thereby reducing the total volume of blood required when analysing both CTCs and ctDNA simultaneously. This is illustrated in Fig. 6.

For these devices to be effective they would need to be:

- Robust and produce highly reproducible results.
- Rapid and not induce any biological change to the sample.
- Operable at the point-of-draw with minimal training required.
- Simple enough to ensure that human error is minimised.
- Free from contaminants.
- Ideally disposable to reduce the chance of sample cross contamination.

Finally, to be clinically implementable, they must provide the best cost-to-benefit ratio to patients and the healthcare system. As blood fractionation and sample preparation are significant parts of the process, devices that support this

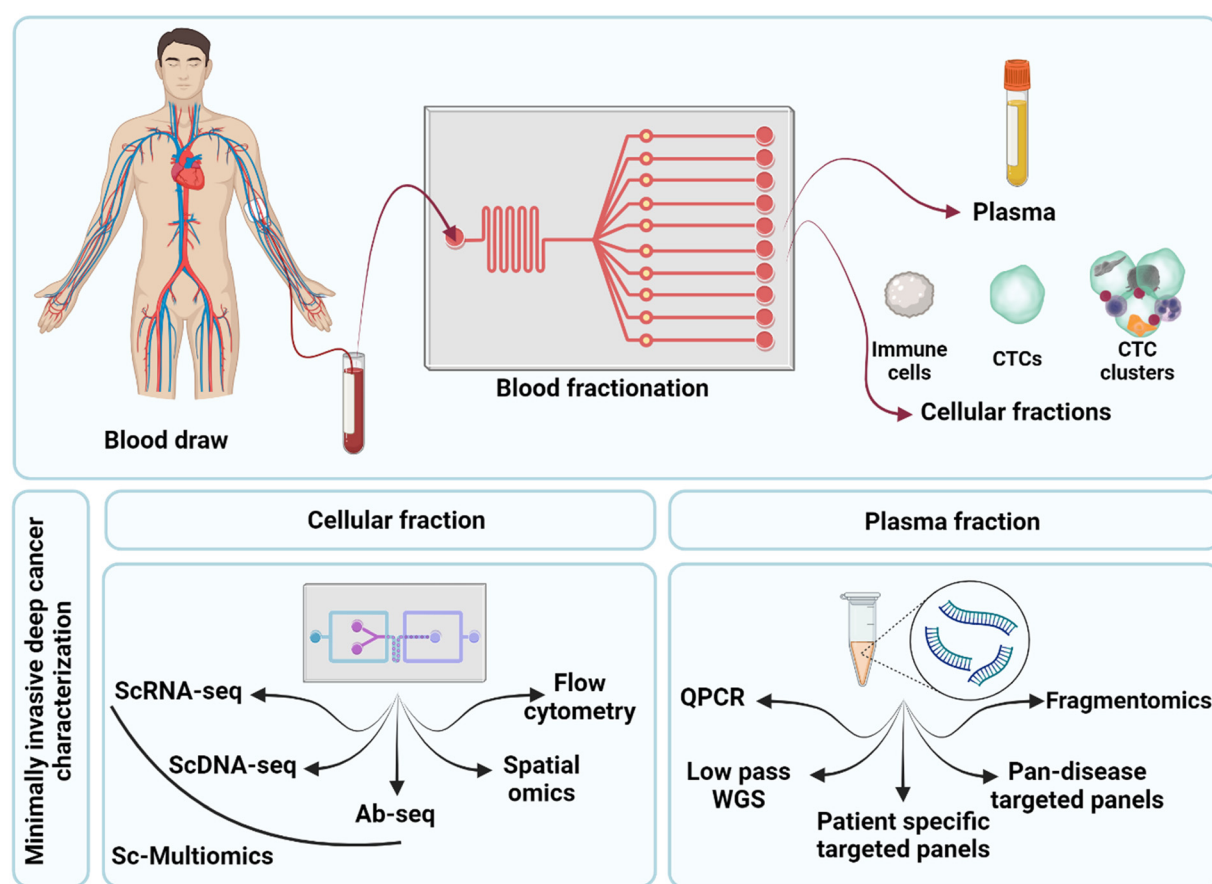


Fig. 6 Workflows for using microfluidics to overcome challenges in liquid biopsy. By enabling the simultaneous separation of plasma and cells from a single blood draw at the point-of-draw, the use of preservatives can be removed, and the cells and ctDNA can be provided in a form compatible with next-generation liquid biopsy approaches.

must also be cost effective. The need for cost-effective methods in liquid biopsy is accentuated by the need to perform these assays at multiple time points during the patient's disease journey.

Here, we have outlined the biological relevance of liquid biopsy approaches in the management of cancer and have proposed a new categorisation approach that we believe helps biologists engage with the complex field of the microfluidic devices that are reshaping our ability to fractionate blood and are set to give rise to new capabilities in liquid biopsy. Finally, through a thorough review of the current state of microfluidics in cancer liquid biopsy, we have identified that many of the current devices are not compatible with multimodal, multiomic analysis. As such, we have proposed several requirements for future devices. We believe that devices allowing rapid and robust point-of-draw fractionation of plasma, CTCs, CTC clusters, and immune cells would provide enormous value to the clinical management of cancer and would therefore have significant impact on the lives of cancer patients.

## Abbreviations

CTC	Circulating tumour cell
SNV	Single nucleotide variant
ctDNA	Circulating tumour DNA
CNA	Copy number aberration
cfDNA	Cell free DNA
NGS	Next generation sequencing
WGS	Whole genome sequencing
DTC	Disseminated tumour cell

## Data availability

No data is available for this review article.

## Author contributions

RS: conceptualisation, formal analysis, investigation, writing – original draft and editing, project administration, visualisation SRB: conceptualisation, writing – original draft, visualisation, investigation, KM: writing – original draft DGO: writing – review & editing, MW: writing – review & editing, supervision DW: writing – review & editing, supervision DJ: writing – review & editing, funding acquisition, supervision.

## Conflicts of interest

The authors declare no conflicts of interest.

## Acknowledgements

DGO is supported by the Elaine Henry Fellowship from the National Breast Cancer Foundation, Australia, IIRS-21-096. RS was supported by funding from Medical Research Futures Fund, Australia (EPCD000015). SRB was supported through generous donations from the Charles Warman foundation,

Australia and Cancer Institute of New South Wales, Australia. The work at Harvard University was supported in part by the National Science Foundation through the Harvard MRSEC (DMR-2011754). We acknowledge the support of the ACRF Child Cancer Liquid Biopsy Program and the Australian Cancer Research Foundation.

## References

- 1 H. Lilja, D. Ulmert and A. J. Vickers, *Nat. Rev. Cancer*, 2008, **8**, 268–278.
- 2 G. L. Perkins, E. D. Slater, G. K. Sanders and J. G. Prichard, *Am. Fam. Physician*, 2003, **68**, 1075–1082.
- 3 X. Q. Chen, M. Stroun, J. L. Magnenat, L. P. Nicod, A. M. Kurt, J. Lyautey, C. Lederrey and P. Anker, *Nat. Med.*, 1996, **2**, 1033–1035.
- 4 H. Nawroz, W. Koch, P. Anker, M. Stroun and D. Sidransky, *Nat. Med.*, 1996, **2**, 1035–1037.
- 5 H. Osumi, E. Shinozaki, K. Yamaguchi and H. Zembutsu, *Sci. Rep.*, 2019, **9**, 17358.
- 6 Y. J. Kim, Y. Kang, J. S. Kim, H. H. Sung, H. G. Jeon, B. C. Jeong, S. I. Seo, S. S. Jeon, H. M. Lee, D. Park, W.-Y. Park and M. Kang, *Sci. Rep.*, 2021, **11**, 5600.
- 7 B. Zhou, K. Xu, X. Zheng, T. Chen, J. Wang, Y. Song, Y. Shao and S. Zheng, *Signal Transduction Targeted Ther.*, 2020, **5**, 144.
- 8 S. Lin, Z. Yu, D. Chen, Z. Wang, J. Miao, Q. Li, D. Zhang, J. Song and D. Cui, *Small*, 2020, **16**, 1903916.
- 9 F. Tian, C. Liu, J. Deng and J. Sun, *Acc. Mater. Res.*, 2022, **3**, 498–510, DOI: [10.1021/accountsmr.1c00276](https://doi.org/10.1021/accountsmr.1c00276).
- 10 B. Lin, Y. Lei, J. Wang, L. Zhu, Y. Wu, H. Zhang, L. Wu, P. Zhang and C. Yang, *Small Methods*, 2021, **5**, 2001131.
- 11 B. M. Szczerba, F. Castro-Giner, M. Vetter, I. Krol, S. Gkountela, J. Landin, M. C. Scheidmann, C. Donato, R. Scherrer, J. Singer, C. Beisel, C. Kurzeder, V. Heinzelmann-Schwarz, C. Rochlitz, W. P. Weber, N. Beerewinkel and N. Aceto, *Nature*, 2019, **566**, 553–557.
- 12 M. Yu, A. Bardia, B. S. Wittner, S. L. Stott, M. E. Smas, D. T. Ting, S. J. Isakoff, J. C. Ciciliano, M. N. Wells, A. M. Shah, K. F. Concannon, M. C. Donaldson, L. V. Sequist, E. Brachtel, D. Sgroi, J. Baselga, S. Ramaswamy, M. Toner, D. A. Haber and S. Maheswaran, *Science*, 2013, **339**, 580–584.
- 13 N. Aceto, A. Bardia, D. T. Miyamoto, M. C. Donaldson, B. S. Wittner, J. A. Spencer, M. Yu, A. Pely, A. Engstrom, H. Zhu, B. W. Brannigan, R. Kapur, S. L. Stott, T. Shioda, S. Ramaswamy, D. T. Ting, C. P. Lin, M. Toner, D. A. Haber and S. Maheswaran, *Cell*, 2014, **158**, 1110–1122.
- 14 K. J. Cheung, V. Padmanaban, V. Silvestri, K. Schipper, J. D. Cohen, A. N. Fairchild, M. A. Gorin, J. E. Verdone, K. J. Pienta, J. S. Bader and A. J. Ewald, *Proc. Natl. Acad. Sci. U. S. A.*, 2016, **113**, E854–E863.
- 15 Z. Yu, H. Chen, J. Ai, Y. Zhu, Y. Li, J. A. Borgia, J.-S. Yang, J. Zhang, B. Jiang, W. Gu and Y. Deng, *Onco Targets Ther.*, 2017, **8**, 107899–107906.



16 Y. Takanashi, T. Kahyo, K. Sekihara, A. Kawase, M. Setou and K. Funai, *Lipids Health Dis.*, 2024, **23**, 154.

17 E. S. Gray, H. Rizos, A. L. Reid, S. C. Boyd, M. R. Pereira, J. Lo, V. Tembe, J. Freeman, J. H. Lee, R. A. Scolyer, K. Siew, C. Lomma, A. Cooper, M. A. Khattak, T. M. Meniawy, G. V. Long, M. S. Carlino, M. Millward and M. Ziman, *Onco Targets Ther.*, 2015, **6**, 42008–42018.

18 H. Cheng, C. Liu, J. Jiang, G. Luo, Y. Lu, K. Jin, M. Guo, Z. Zhang, J. Xu, L. Liu, Q. Ni and X. Yu, *Int. J. Cancer*, 2017, **140**, 2344–2350.

19 F. Diehl, K. Schmidt, M. A. Choti, K. Romans, S. Goodman, M. Li, K. Thornton, N. Agrawal, L. Sokoll, S. A. Szabo, K. W. Kinzler, B. Vogelstein and L. A. Diaz, Jr., *Nat. Med.*, 2008, **14**, 985–990.

20 G. Ledergor, A. Weiner, M. Zada, S. Y. Wang, Y. C. Cohen, M. E. Gatt, N. Snir, H. Magen, M. Koren-Michowitz, K. Herzog-Tzarfaty, H. Keren-Shaul, C. Bornstein, R. Rotkopf, I. Yofe, E. David, V. Yellapantula, S. Kay, M. Salai, D. Ben Yehuda, A. Nagler, L. Shvidel, A. Orr-Urtreger, K. B. Halpern, S. Itzkovitz, O. Landgren, J. San-Miguel, B. Paiva, J. J. Keats, E. Papaemmanuil, I. Avivi, G. I. Barbash, A. Tanay and I. Amit, *Nat Med.*, 2018, **24**, 1867–1876.

21 S. D. Wit, G. V. Dalum, A. T. M. Lenferink, A. G. J. Tibbe, T. J. N. Hiltermann, H. J. M. Groen, C. J. M. van Rijn and L. W. M. M. Terstappen, *Sci. Rep.*, 2015, **5**, 12270.

22 J. M. Riedl, S. O. Hasenleithner, G. Pregartner, L. Scheipner, F. Posch, K. Groller, K. Kashofer, S. W. Jahn, T. Bauernhofer, M. Pichler, H. Stöger, A. Berghold, G. Hoefler, M. R. Speicher, E. Heitzer and A. Gerger, *Ther. Adv. Med. Oncol.*, 2021, **13**, 1758835920987658.

23 C. L. Hodgkinson, C. J. Morrow, Y. Li, R. L. Metcalf, D. G. Rothwell, F. Trapani, R. Polanski, D. J. Burt, K. L. Simpson, K. Morris, S. D. Pepper, D. Nonaka, A. Greystoke, P. Kelly, B. Bola, M. G. Krebs, J. Antonello, M. Ayub, S. Faulkner, L. Priest, L. Carter, C. Tate, C. J. Miller, F. Blackhall, G. Brady and C. Dive, *Nat. Med.*, 2014, **20**, 897–903.

24 C. Abbosh, N. J. Birkbak, G. A. Wilson, M. Jamal-Hanjani, T. Constantin, R. Salari, J. Le Quesne, D. A. Moore, S. Veeriah, R. Rosenthal, T. Marafioti, E. Kirkizlar, T. B. K. Watkins, N. McGranahan, S. Ward, L. Martinson, J. Riley, F. Fraioli, M. Al Bakir, E. Gronroos, F. Zambrana, R. Endozo, W. L. Bi, F. M. Fennelly, N. Sponer, D. Johnson, J. Laycock, S. Shafi, J. Czyzewska-Khan, A. Rowan, T. Chambers, N. Matthews, S. Turajlic, C. Hiley, S. M. Lee, M. D. Forster, T. Ahmad, M. Falzon, E. Borg, D. Lawrence, M. Hayward, S. Kolvekar, N. Panagiotopoulos, S. M. Janes, R. Thakrar, A. Ahmed, F. Blackhall, Y. Summers, D. Hafez, A. Naik, A. Ganguly, S. Kareth, R. Shah, L. Joseph, A. Marie Quinn, P. A. Crosbie, B. Naidu, G. Middleton, G. Langman, S. Trotter, M. Nicolson, H. Remmen, K. Kerr, M. Chetty, L. Gomersall, D. A. Fennell, A. Nakas, S. Rathinam, G. Anand, S. Khan, P. Russell, V. Ezhil, B. Ismail, M. Irvin-Sellers, V. Prakash, J. F. Lester, M. Kornaszewska, R. Attanoos, H. Adams, H. Davies, D. Oukrif, A. U. Akarca, J. A. Hartley, H. L. Lowe, S. Lock, N. Iles, H. Bell, Y. Ngai, G. Elgar, Z. Szallasi, R. F. Schwarz, J. Herrero, A. Stewart, S. A. Quezada, K. S. Peggs, P. Van Loo, C. Dive, C. J. Lin, M. Rabinowitz, H. Aerts, A. Hackshaw, J. A. Shaw, B. G. Zimmermann, T. R. Consortium, P. Consortium and C. Swanton, *Nature*, 2017, **545**, 446–451.

25 M. Murtaza, S. J. Dawson, D. W. Tsui, D. Gale, T. Forshaw, A. M. Piskorz, C. Parkinson, S. F. Chin, Z. Kingsbury, A. S. Wong, F. Marass, S. Humphray, J. Hadfield, D. Bentley, T. M. Chin, J. D. Brenton, C. Caldas and N. Rosenfeld, *Nature*, 2013, **497**, 108–112.

26 S. L. Kong, X. Liu, S. J. Tan, J. A. Tai, L. Y. Phua, H. M. Poh, T. Yeo, Y. W. Chua, Y. X. Haw, W. H. Ling, R. C. H. Ng, T. J. Tan, K. W. J. Loh, D. S.-W. Tan, Q. S. Ng, M. K. Ang, C. K. Toh, Y. F. Lee, C. T. Lim, T. K. H. Lim, A. M. Hillmer, Y. S. Yap and W.-T. Lim, *Front. Oncol.*, 2021, **11**, 698551, DOI: [10.3389/fpone.2021.698551](https://doi.org/10.3389/fpone.2021.698551).

27 Y. Wang, L. Guo, L. Feng, W. Zhang, T. Xiao, X. Di, G. Chen and K. Zhang, *Oncol. Rep.*, 2018, **39**, 2147–2159.

28 E. S. Antonarakis, C. Lu, H. Wang, B. Luber, M. Nakazawa, J. C. Roeser, Y. Chen, T. A. Mohammad, Y. Chen, H. L. Fedor, T. L. Lotan, Q. Zheng, A. M. De Marzo, J. T. Isaacs, W. B. Isaacs, R. Nadal, C. J. Paller, S. R. Denmeade, M. A. Carducci, M. A. Eisenberger and J. Luo, *N. Engl. J. Med.*, 2014, **371**, 1028–1038.

29 T. T. Kwan, A. Bardia, L. M. Spring, A. Giobbie-Hurder, M. Kalinich, T. Dubash, T. Sundaresan, X. Hong, J. A. LiCausi, U. Ho, E. J. Silva, B. S. Wittner, L. V. Sequist, R. Kapur, D. T. Miyamoto, M. Toner, D. A. Haber and S. Maheswaran, *Cancer Discovery*, 2018, **8**, 1286–1299.

30 A. Zviran, R. C. Schulman, M. Shah, S. T. K. Hill, S. Deochand, C. C. Khamnei, D. Maloney, K. Patel, W. Liao, A. J. Widman, P. Wong, M. K. Callahan, G. Ha, S. Reed, D. Rotem, D. Frederick, T. Sharova, B. Miao, T. Kim, G. Gydush, J. Rhoades, K. Y. Huang, N. D. Omans, P. O. Bolan, A. H. Lipsky, C. Ang, M. Malbari, C. F. Spinelli, S. Kazancioglu, A. M. Runnels, S. Fennessey, C. Stolte, F. Gaiti, G. G. Inghirami, V. Adalsteinsson, B. Houck-Loomis, J. Ishii, J. D. Wolchok, G. Boland, N. Robine, N. K. Altorki and D. A. Landau, *Nat. Med.*, 2020, **26**, 1114–1124, DOI: [10.1038/s41591-020-0915-3](https://doi.org/10.1038/s41591-020-0915-3).

31 J. C. M. Wan, K. Heider, D. Gale, S. Murphy, E. Fisher, F. Mouliere, A. Ruiz-Valdepenas, A. Santonja, J. Morris, D. Chandrananda, A. Marshall, A. B. Gill, P. Y. Chan, E. Barker, G. Young, W. N. Cooper, I. Hudecova, F. Marass, R. Mair, K. M. Brindle, G. D. Stewart, J. E. Abraham, C. Caldas, D. M. Rassl, R. C. Rintoul, C. Alifrangis, M. R. Middleton, F. A. Gallagher, C. Parkinson, A. Durrani, U. McDermott, C. G. Smith, C. Massie, P. G. Corrie and N. Rosenfeld, *Sci. Transl. Med.*, 2020, **12**, eaaz8084, DOI: [10.1126/scitranslmed.aaz8084](https://doi.org/10.1126/scitranslmed.aaz8084).

32 J. J. Szymanski, R. T. Sundby, P. A. Jones, D. Srihari, N. Earland, P. K. Harris, W. Feng, F. Qaium, H. Lei, D. Roberts, M. Landeau, J. Bell, Y. Huang, L. Hoffman, M. Spencer, M. B. Spraker, L. Ding, B. C. Widemann, J. F. Shern, A. C. Hirbe and A. A. Chaudhuri, *PLoS Med.*, 2021, **18**, e1003734.





33 F. Mouliere, D. Chandrananda, A. M. Piskorz, E. K. Moore, J. Morris, L. B. Ahlborn, R. Mair, T. Goranova, F. Marass, K. Heider, J. C. M. Wan, A. Supernat, I. Hudecova, I. Gounaris, S. Ros, M. Jimenez-Linan, J. Garcia-Corbacho, K. Patel, O. Østrup, S. Murphy, M. D. Eldridge, D. Gale, G. D. Stewart, J. Burge, W. N. Cooper, M. S. van der Heijden, C. E. Massie, C. Watts, P. Corrie, S. Pacey, K. M. Brindle, R. D. Baird, M. Mau-Sørensen, C. A. Parkinson, C. G. Smith, J. D. Brenton and N. Rosenfeld, *Sci. Transl. Med.*, 2018, **10**, eaat4921.

34 A. R. Thierry, *Cell Genomics*, 2023, **3**, 100242.

35 S. C. Ding and Y. M. D. Lo, *Diagnostics*, 2022, **12**, 978, DOI: [10.3390/diagnostics12040978](https://doi.org/10.3390/diagnostics12040978).

36 C. Abbosh, A. M. Frankell, T. Harrison, J. Kisistok, A. Garnett, L. Johnson, S. Veeriah, M. Moreau, A. Chesh, T. L. Chaunzwa, J. Weiss, M. R. Schroeder, S. Ward, K. Grigoriadis, A. Shahpurwalla, K. Litchfield, C. Puttik, D. Biswas, T. Karasaki, J. R. M. Black, C. Martínez-Ruiz, M. A. Bakir, O. Pich, T. B. K. Watkins, E. L. Lim, A. Huebner, D. A. Moore, N. Godin-Heymann, A. L'Hernault, H. Bye, A. Odell, P. Roberts, F. Gomes, A. J. Patel, E. Manzano, C. T. Hiley, N. Carey, J. Riley, D. E. Cook, D. Hodgson, D. Stetson, J. C. Barrett, R. M. Kortlever, G. I. Evan, A. Hackshaw, R. D. Daber, J. A. Shaw, H. Aerts, A. Licon, J. Stahl, M. Jamal-Hanjani, N. J. Birkbak, N. McGranahan and C. Swanton, *Nature*, 2023, **616**, 553–562.

37 K. Chen, F. Yang, H. Shen, C. Wang, X. Li, O. Chervova, S. Wu, F. Qiu, D. Peng, X. Zhu, S. Chuai, S. Beck, N. Kanu, D. Carbone, Z. Zhang and J. Wang, *Cancer Cell*, 2023, **41**, 1749–1762, e1746.

38 S.-B. Ryoo, S. Heo, Y. Lim, W. Lee, S. H. Cho, J. Ahn, J.-K. Kang, S. Y. Kim, H.-P. Kim, D. Bang, S.-B. Kang, C. S. Yu, S. T. Oh, J. W. Park, S.-Y. Jeong, Y.-J. Kim, K. J. Park, S.-W. Han and T.-Y. Kim, *Br. J. Cancer*, 2023, **129**, 374–381.

39 S. B. Ng, C. Chua, M. Ng, A. Gan, P. S. Y. Poon, M. Teo, C. Fu, W. Q. Leow, K. H. Lim, A. Chung, S.-L. Koo, S. P. Choo, D. Ho, S. Rozen, P. Tan, M. Wong, W. F. Burkholder and I. B. Tan, *Sci. Rep.*, 2017, **7**, 40737.

40 A. Santonja, W. N. Cooper, M. D. Eldridge, P. A. W. Edwards, J. A. Morris, A. R. Edwards, H. Zhao, K. Heider, D. L. Couturier, A. Vijayaraghavan, P. Mennea, E. J. Ditter, C. G. Smith, C. Bourne, R. Manzano García, O. M. Rueda, E. Beddowes, H. Biggs, S. J. Sammut, N. Rosenfeld, C. Caldas, J. E. Abraham and D. Gale, *EMBO Mol. Med.*, 2023, **15**, e16505.

41 M. Stoeckius, C. Hafemeister, W. Stephenson, B. Houck-Loomis, P. K. Chattopadhyay, H. Swerdlow, R. Satija and P. Smibert, *Nat. Methods*, 2017, **14**, 865–868.

42 E. Z. Macosko, A. Basu, R. Satija, J. Nemesh, K. Shekhar, M. Goldman, I. Tirosh, A. R. Bialas, N. Kamitaki, E. M. Martersteck, J. J. Trombetta, D. A. Weitz, J. R. Sanes, A. K. Shalek, A. Regev and S. A. McCarroll, *Cell*, 2015, **161**, 1202–1214.

43 R. Zilionis, J. Nainys, A. Veres, V. Savova, D. Zemmour, A. M. Klein and L. Mazutis, *Nat. Protoc.*, 2017, **12**, 44–73.

44 M. Cristofanilli, G. T. Budd, M. J. Ellis, A. Stopeck, J. Matera, M. C. Miller, J. M. Reuben, G. V. Doyle, W. J. Allard, L. W. Terstappen and D. F. Hayes, *N. Engl. J. Med.*, 2004, **351**, 781–791.

45 N. Aceto, *Onco Targets Ther*, 2019, **10**, 2658–2659.

46 J. G. Lohr, V. A. Adalsteinsson, K. Cibulskis, A. D. Choudhury, M. Rosenberg, P. Cruz-Gordillo, J. M. Francis, C. Z. Zhang, A. K. Shalek, R. Satija, J. J. Trombetta, D. Lu, N. Tallapragada, N. Tahirova, S. Kim, B. Blumenstiel, C. Sougnez, A. Lowe, B. Wong, D. Auclair, E. M. Van Allen, M. Nakabayashi, R. T. Lis, G. S. Lee, T. Li, M. S. Chabot, A. Ly, M. E. Taplin, T. E. Clancy, M. Loda, A. Regev, M. Meyerson, W. C. Hahn, P. W. Kantoff, T. R. Golub, G. Getz, J. S. Boehm and J. C. Love, *Nat. Biotechnol.*, 2014, **32**, 479–484.

47 V. Cappelletti, E. Verzoni, R. Ratta, M. Vismara, M. Silvestri, R. Montone, P. Miodini, C. Reduzzi, M. Claps, P. Sepe, M. G. Daidone and G. Procopio, *Int. J. Mol. Sci.*, 2020, **21**, 1475, DOI: [10.3390/ijms21041475](https://doi.org/10.3390/ijms21041475).

48 M. Chimonidou, A. Strati, A. Tzitzira, G. Sotiropoulou, N. Malamos, V. Georgoulias and E. S. Lianidou, *Clin. Chem.*, 2011, **57**, 1169–1177.

49 L. Zhao, X. Wu, J. Zheng and D. Dong, *Oncogene*, 2021, **40**, 1884–1895.

50 S. Mastoraki, A. Strati, E. Tzanikou, M. Chimonidou, E. Politaki, A. Voutsina, A. Psyrra, V. Georgoulias and E. Lianidou, *Clin. Cancer Res.*, 2018, **24**, 1500–1510.

51 S. Gkountela, F. Castro-Giner, B. M. Szczerba, M. Vetter, J. Landin, R. Scherrer, I. Krol, M. C. Scheidmann, C. Beisel, C. U. Stirnimann, C. Kurzeder, V. Heinzelmann-Schwarz, C. Rochlitz, W. P. Weber and N. Aceto, *Cell*, 2019, **176**(98–112), e114.

52 I. Krol, F. Castro-Giner, M. Maurer, S. Gkountela, B. M. Szczerba, R. Scherrer, N. Coleman, S. Carreira, F. Bachmann, S. Anderson, M. Engelhardt, H. Lane, T. R. J. Evans, R. Plummer, R. Kristeleit, J. Lopez and N. Aceto, *Br. J. Cancer*, 2018, **119**, 487–491.

53 A. R. Thierry, *Cell Genomics*, 2023, **3**(1), 100242.

54 S. A. Leon, B. Shapiro, D. M. Sklaroff and M. J. Yaros, *Cancer Res.*, 1977, **37**, 646–650.

55 F. Diehl, M. Li, Y. He, K. W. Kinzler, B. Vogelstein and D. Dressman, *Nat. Methods*, 2006, **3**, 551–559.

56 R. Jiang, Y. T. Lu, H. Ho, B. Li, J. F. Chen, M. Lin, F. Li, K. Wu, H. Wu, J. Lichterman, H. Wan, C. L. Lu, W. OuYang, M. Ni, L. Wang, G. Li, T. Lee, X. Zhang, J. Yang, M. Rettig, L. W. Chung, H. Yang, K. C. Li, Y. Hou, H. R. Tseng, S. Hou, X. Xu, J. Wang and E. M. Posadas, *Onco Targets Ther*, 2015, **6**, 44781–44793.

57 H. Peng, L. Lu, Z. Zhou, J. Liu, D. Zhang, K. Nan, X. Zhao, F. Li, L. Tian, H. Dong and Y. Yao, *Genes*, 2019, **10**, 926.

58 T. E. Liggett, A. A. Melnikov, J. R. Marks and V. V. Levenson, *Int. J. Cancer*, 2011, **128**, 492–499.

59 F. Nassiri, A. Chakravarthy, S. Feng, S. Y. Shen, R. Nejad, J. A. Zuccato, M. R. Voisin, V. Patil, C. Horbinski, K. Aldape, G. Zadeh and D. D. De Carvalho, *Nat. Med.*, 2020, **26**, 1044–1047.

60 N. C. Turner, B. Kingston, L. S. Kilburn, S. Kernaghan, A. M. Wardley, I. R. Macpherson, R. D. Baird, R. Roylance, P. Stephens, O. Oikonomidou, J. P. Braybrooke, M. Tuthill,

J. Abraham, M. C. Winter, H. Bye, M. Hubank, H. Gevensleben, R. Cutts, C. Snowdon, D. Rea, D. Cameron, A. Shaaban, K. Randle, S. Martin, K. Wilkinson, L. Moretti, J. M. Bliss and A. Ring, *Lancet Oncol.*, 2020, **21**, 1296–1308.

61 F. Cimmino, V. A. Lasorsa, S. Vetrella, A. Iolascon and M. Capasso, *Front. Oncol.*, 2020, **10**, 596191, DOI: [10.3389/fonc.2020.596191](https://doi.org/10.3389/fonc.2020.596191).

62 S. Bang, D. Won, S. Shin, K. S. Cho, J. W. Park, J. Lee, Y. D. Choi, S. Kang, S. T. Lee, J. R. Choi and H. Han, *Cancers*, 2023, **15**, 3998, DOI: [10.3390/cancers15153998](https://doi.org/10.3390/cancers15153998).

63 M. Kohli, W. Tan, T. Zheng, A. Wang, C. Montesinos, C. Wong, P. Du, S. Jia, S. Yadav, L. G. Horvath, K. L. Mahon, E. M. Kwan, H. Fettke, J. Yu and A. A. Azad, *EBioMedicine*, 2020, **54**, 102728, DOI: [10.1016/j.ebiom.2020.102728](https://doi.org/10.1016/j.ebiom.2020.102728).

64 J. Tie, Y. Wang, C. Tomasetti, L. Li, S. Springer, I. Kinde, N. Silliman, M. Tacey, H.-L. Wong, M. Christie, S. Kosmider, I. Skinner, R. Wong, M. Steel, B. Tran, J. Desai, I. Jones, A. Haydon, T. Hayes, T. J. Price, R. L. Strausberg, L. A. Diaz, N. Papadopoulos, K. W. Kinzler, B. Vogelstein and P. Gibbs, *Sci. Transl. Med.*, 2016, **8**, 346ra392-346ra392.

65 R. C. Fitzgerald, A. C. Antoniou, L. Fruk and N. Rosenfeld, *Nat. Med.*, 2022, **28**, 666–677.

66 Y.-M. Yeh, P.-C. Lin, C.-T. Lee, S.-H. Chen, B.-W. Lin, S.-C. Lin, P.-C. Chen, R.-H. Chan and M.-R. Shen, *Mol. Cancer*, 2020, **19**, 150.

67 S. Nikolaev, L. Lemmens, T. Koessler, J.-L. Blouin and T. Nouspikel, *Anal. Biochem.*, 2018, **542**, 34–39.

68 Y. Zhao, Y. Li, P. Chen, S. Li, J. Luo and H. Xia, *J. Clin. Lab. Anal.*, 2019, **33**, e22670–e22670.

69 F. Mouliere and N. Rosenfeld, *Proc. Natl. Acad. Sci. U. S. A.*, 2015, **112**, 3178–3179.

70 T. R. Ashworth, *Aust. J. Med.*, 1869, **14**, 146–147.

71 T. P. Leitão, P. Corredeira, S. Kucharczak, M. Rodrigues, P. Piairo, C. Rodrigues, P. Alves, A. M. Cavaco, M. Miranda, M. Antunes, J. Ferreira, J. Palma Reis, T. Lopes, L. Diéguez and L. Costa, *Int. J. Mol. Sci.*, 2023, **24**, 8404.

72 F. Jin, L. Zhu, J. Shao, M. Yakoub, L. Schmitt, C. Reißfelder, S. Loges, A. Benner and S. Schölch, *Eur. Respir. J.*, 2022, **31**, 220151.

73 J. Müller Bark, A. Kulasinghe, G. Hartel, P. Leo, M. E. Warkiani, R. L. Jeffree, B. Chua, B. W. Day and C. Punyadeera, *Front. Oncol.*, 2021, **11**, 681130, DOI: [10.3389/fonc.2021.681130](https://doi.org/10.3389/fonc.2021.681130).

74 M. Kojima, T. Harada, T. Fukazawa, S. Kurihara, R. Touge, I. Saeki, S. Takahashi and E. Hiyama, *Cancer Sci.*, 2023, **114**, 1616–1624.

75 M. Hayashi, P. Zhu, G. McCarty, C. F. Meyer, C. A. Pratillas, A. Levin, C. D. Morris, C. M. Albert, K. W. Jackson, C.-M. Tang and D. M. Loeb, *Onco Targets Ther.*, 2017, **8**, 78965–78977, DOI: [10.18632/oncotarget.20697](https://doi.org/10.18632/oncotarget.20697).

76 C. Paoletti, A. K. Cani, J. M. Larios, D. H. Hovelson, K. Aung, E. P. Darga, E. M. Cannell, P. J. Baratta, C.-J. Liu, D. Chu, M. Yazdani, A. R. Blevins, V. Sero, N. Tokudome, D. G. Thomas, C. Gersch, A. F. Schott, Y.-M. Wu, R. Lonigro, D. R. Robinson, A. M. Chinnaiyan, F. Z. Bischoff, M. D. Johnson, B. H. Park, D. F. Hayes, J. M. Rae and S. A. Tomlins, *Cancer Res.*, 2018, **78**, 1110–1122.

77 D. Ramsköld, S. Luo, Y.-C. Wang, R. Li, Q. Deng, O. R. Faridani, G. A. Daniels, I. Khrebdukova, J. F. Loring, L. C. Laurent, G. P. Schrot and R. Sandberg, *Nat. Biotechnol.*, 2012, **30**, 777–782.

78 G. T. Budd, M. Cristofanilli, M. J. Ellis, A. Stopeck, E. Borden, M. C. Miller, J. Matera, M. Repollet, G. V. Doyle, L. W. Terstappen and D. F. Hayes, *Clin. Cancer Res.*, 2006, **12**, 6403–6409.

79 M. G. Krebs, J.-M. Hou, T. H. Ward, F. H. Blackhall and C. Dive, *Ther. Adv. Med. Oncol.*, 2010, **2**, 351–365.

80 S. Pang, H. Li, S. Xu, L. Feng, X. Ma, Y. Chu, B. Zou, S. Wang and G. Zhou, *Sci. Rep.*, 2021, **11**, 13441.

81 D. W. Ross, L. H. Ayscue, J. Watson and S. A. Bentley, *Am. J. Clin. Pathol.*, 1988, **90**, 262–267.

82 M. Diez-Silva, M. Dao, J. Han, C. T. Lim and S. Suresh, *MRS Bull.*, 2010, **35**, 382–388.

83 H. W. Hou, A. A. S. Bhagat, W. C. Lee, S. Huang, J. Han and C. T. Lim, *Micromachines*, 2011, **2**, 319–343.

84 W. J. Allard, J. Matera, M. C. Miller, M. Repollet, M. C. Connelly, C. Rao, A. G. J. Tibbe, J. W. Uhr and L. W. M. M. Terstappen, *Clin. Cancer Res.*, 2004, **10**, 6897–6904.

85 S. L. Stott, R. J. Lee, S. Nagrath, M. Yu, D. T. Miyamoto, L. Ulkus, E. J. Inserra, M. Ulman, S. Springer, Z. Nakamura, A. L. Moore, D. I. Tsukrov, M. E. Kempner, D. M. Dahl, C.-L. Wu, A. J. Iafrate, M. R. Smith, R. G. Tompkins, L. V. Sequist, M. Toner, D. A. Haber and S. Maheswaran, *Sci. Transl. Med.*, 2010, **2**, 25ra23.

86 S. Meng, D. Tripathy, E. P. Frenkel, S. Shete, E. Z. Naftalis, J. F. Huth, P. D. Beitsch, M. Leitch, S. Hoover, D. Euhus, B. Haley, L. Morrison, T. P. Fleming, D. Herlyn, L. W. M. M. Terstappen, T. Fehm, T. F. Tucker, N. Lane, J. Wang and J. W. Uhr, *Clin. Cancer Res.*, 2004, **10**, 8152–8162.

87 R. M. Trigg, L. J. Martinson, S. Parpart-Li and J. A. Shaw, *Heliyon*, 2018, **4**, e00699, DOI: [10.1016/j.heliyon.2018.e00699](https://doi.org/10.1016/j.heliyon.2018.e00699).

88 P. Sethu, M. Anahtar, L. L. Moldawer, R. G. Tompkins and M. Toner, *Anal. Chem.*, 2004, **76**, 6247–6253.

89 S. Miltenyi, W. Muller, W. Weichel and A. Radbruch, *Cytometry*, 1990, **11**, 231–238.

90 H. R. Hulett, W. A. Bonner, J. Barrett and L. A. Herzenberg, *Science*, 1969, **166**, 747–749.

91 L. A. Herzenberg, R. G. Sweet and L. A. Herzenberg, *Sci. Am.*, 1976, **234**, 108–118.

92 J. L. Sherwood, C. Corcoran, H. Brown, A. D. Sharpe, M. Musilova and A. Kohlmann, *PLoS One*, 2016, **11**, e0150197.

93 M. Fleischhacker and B. Schmidt, *J. Lab. Med.*, 2020, **44**, 117–142.

94 M. A. Kerachian, M. Azghandi, S. Mozaffari-Jovin and A. R. Thierry, *Clin. Epigenet.*, 2021, **13**, 193.

95 A. Ward, Gahlawat, J. Lenhardt, T. Witte, D. Keitel, A. Kaufhold, K. K. Maass, K. W. Pajtler, C. Sohn and S. Schott, *Int. J. Mol. Sci.*, 2019, **20**, 704.

96 L. Sorber, K. Zwaenepoel, J. Jacobs, K. De Winne, S. Goethals, P. Reclusa, K. Van Casteren, E. Augustus, F. Lardon, G. Roeyen, M. Peeters, J. Van Meerbeeck, C. Rolfo and P. Pauwels, *Cancers*, 2019, **11**, 458.



97 D. Grolz, S. Hauch, M. Schlumpberger, K. Guenther, T. Voss, M. Sprenger-Haussels and U. Oelmuller, *Curr. Pathobiol. Rep.*, 2018, **6**, 275–286.

98 H. Cho, J. Kim, H. Song, K. Y. Sohn, M. Jeon and K.-H. Han, *Analyst*, 2018, **143**, 2936–2970.

99 L. Descamps, D. Le Roy and A. L. Deman, *Int. J. Mol. Sci.*, 2022, **23**, 1981, DOI: [10.3390/ijms23041981](https://doi.org/10.3390/ijms23041981).

100 S.-J. Hao, Y. Wan, Y.-Q. Xia, X. Zou and S.-Y. Zheng, *Adv. Drug Delivery Rev.*, 2018, **125**, 3–20.

101 T. A. Crowley and V. Pizziconi, *Lab Chip*, 2005, **5**, 922–929.

102 J. A. Davis, D. W. Inglis, K. J. Morton, D. A. Lawrence, L. R. Huang, S. Y. Chou, J. C. Sturm and R. H. Austin, *Proc. Natl. Acad. Sci. U. S. A.*, 2006, **103**, 14779–14784.

103 S. Yang, A. Undar and J. D. Zahn, *Lab Chip*, 2006, **6**, 871–880.

104 S. Tripathi, Y. V. Kumar, A. Agrawal, A. Prabhakar and S. S. Joshi, *Sci. Rep.*, 2016, **6**, 26749.

105 A. Lenshof, A. Ahmad-Tajudin, K. Järås, A.-M. Swärd-Nilsson, L. Åberg, G. Marko-Varga, J. Malm, H. Lilja and T. Laurell, *Anal. Chem.*, 2009, **81**, 6030–6037.

106 J. S. Shim, A. W. Browne and C. H. Ahn, *Biomed. Microdevices*, 2010, **12**, 949–957.

107 M. G. Lee, S. Choi, H.-J. Kim, H. K. Lim, J.-H. Kim, N. Huh and J.-K. Park, *Appl. Phys. Lett.*, 2011, **98**, 253702.

108 C. Szydzik, K. Khoshmanesh, A. Mitchell and C. Karnutsch, *Biomicrofluidics*, 2015, **9**, 064120.

109 X. Xing, M. He, H. Qiu and L. Yobas, *Anal. Chem.*, 2016, **88**, 5197–5204.

110 H. Jang, M. R. Haq, J. Ju, Y. Kim, S.-m. Kim and J. Lim, *Micromachines*, 2017, **8**, 67.

111 C.-J. Kim, J. Park, V. Sunkara, T.-H. Kim, Y. Lee, K. Lee, M.-H. Kim and Y.-K. Cho, *Lab Chip*, 2018, **18**, 1320–1329.

112 Q. Gao, Y. Chang, Q. Deng and H. You, *Anal. Methods*, 2020, **12**, 2560–2570.

113 W. Brakewood, K. Lee, L. Schneider, N. Lawandy and A. Tripathi, *Front. Lab. Chip. Technol.*, 2022, **1**, 1051552, DOI: [10.3389/flct.2022.1051552](https://doi.org/10.3389/flct.2022.1051552).

114 E. Sollier, M. Cubizolles, Y. Fouillet and J.-L. Achard, *Biomed. Microdevices*, 2010, **12**, 485–497.

115 D. H. Kuan, C. C. Wu, W. Y. Su and N. T. Huang, *Sci. Rep.*, 2018, **8**, 15345.

116 Y. Liu, W. Zhao, R. Cheng, J. Hodgson, M. Egan, C. N. C. Pope, P. G. Nikolinakos and L. Mao, *Lab Chip*, 2021, **21**, 3583–3597.

117 M. Boya, T. Ozkaya-Ahmadov, B. E. Swain, C.-H. Chu, N. Asmare, O. Civelekoglu, R. Liu, D. Lee, S. Tobia, S. Biliya, L. D. McDonald, B. Nazha, O. Kucuk, M. G. Sanda, B. B. Benigno, C. S. Moreno, M. A. Bilen, J. F. McDonald and A. F. Sarioglu, *Nat. Commun.*, 2022, **13**, 3385.

118 H. J. Woo, S. H. Kim, H. J. Kang, S. H. Lee, S. J. Lee, J. M. Kim, O. Gurel, S. Y. Kim, H. R. Roh, J. Lee, Y. Park, H. Y. Shin, Y. I. Shin, S. M. Lee, S. Y. Oh, Y. Z. Kim, J. I. Chae, S. Lee, M. H. Hong, B. C. Cho, E. S. Lee, K. Pantel, H. R. Kim and M. S. Kim, *Theranostics*, 2022, **12**, 3676–3689.

119 Z. Zhu, H. Ren, D. Wu, Z. Ni and N. Xiang, *Microsyst. Nanoeng.*, 2024, **10**, 36.

120 W. Pakhira, R. Kumar and K. M. Ibrahim, *Chem. Eng. Sci.*, 2023, **275**, 118724.

121 V. Omrani, M. Z. Targhi, F. Rahbarizadeh and R. Nosrati, *Sci. Rep.*, 2023, **13**, 3213.

122 Y. Lu, S. Yue, M. Liang, T. Wang, R. Wang, Z. Chen and J. Fang, *Sens. Actuators, B*, 2023, **393**, 134174.

123 R. M. Mohamadi, J. D. Besant, A. Mepham, B. Green, L. Mahmoudian, T. Gibbs, I. Ivanov, A. Malvea, J. Stojcic, A. L. Allan, L. E. Lowes, E. H. Sargent, R. K. Nam and S. O. Kelley, *Angew. Chem., Int. Ed.*, 2015, **54**, 139–143.

124 M. C. Miller, P. S. Robinson, C. Wagner and D. J. O'Shannessy, *Cytometry, Part A*, 2018, **93**, 1234–1239.

125 L. Xu, X. Mao, A. Imrali, F. Syed, K. Mutsvangwa, D. Berney, P. Cathcart, J. Hines, J. Shamash and Y. J. Lu, *PLoS One*, 2015, **10**, e0138032.

126 M. E. Warkiani, G. Guan, K. B. Luan, W. C. Lee, A. A. Bhagat, P. K. Chaudhuri, D. S. Tan, W. T. Lim, S. C. Lee, P. C. Chen, C. T. Lim and J. Han, *Lab Chip*, 2014, **14**, 128–137.

127 S. Ribeiro-Samy, M. I. Oliveira, T. Pereira-Veiga, L. Muinelo-Romay, S. Carvalho, J. Gaspar, P. P. Freitas, R. López-López, C. Costa and L. Diéguez, *Sci. Rep.*, 2019, **9**, 8032.

128 R. Riahi, P. Gogoi, S. Sepehri, Y. Zhou, K. Handique, J. Godsey and Y. Wang, *Int. J. Oncol.*, 2014, **44**, 1870–1878.

129 P. Gogoi, S. Sepehri, Y. Zhou, M. A. Gorin, C. Paolillo, E. Capoluongo, K. Gleason, A. Payne, B. Boniface, M. Cristofanilli, T. M. Morgan, P. Fortina, K. J. Pienta, K. Handique and Y. Wang, *PLoS One*, 2016, **11**, e0147400.

130 E. Sollier, D. E. Go, J. Che, D. R. Gossett, S. O'Byrne, W. M. Weaver, N. Kummer, M. Rettig, J. Goldman, N. Nickols, S. McCloskey, R. P. Kulkarni and D. Di Carlo, *Lab Chip*, 2014, **14**, 63–77.

131 V. Murlidhar, M. Zeinali, S. Grabauskiene, M. Ghannad-Rezaie, M. S. Wicha, D. M. Simeone, N. Ramnath, R. M. Reddy and S. Nagrath, *Small*, 2014, **10**, 4895–4904.

132 A. F. Sarioglu, N. Aceto, N. Kojic, M. C. Donaldson, M. Zeinali, B. Hamza, A. Engstrom, H. Zhu, T. K. Sundaresan, D. T. Miyamoto, X. Luo, A. Bardia, B. S. Wittner, S. Ramaswamy, T. Shioda, D. T. Ting, S. L. Stott, R. Kapur, S. Maheswaran, D. A. Haber and M. Toner, *Nat. Methods*, 2015, **12**, 685–691.

133 Y. T. Lu, L. Zhao, Q. Shen, M. A. Garcia, D. Wu, S. Hou, M. Song, X. Xu, W. H. Ouyang, W. W. Ouyang, J. Lichterman, Z. Luo, X. Xuan, J. Huang, L. W. Chung, M. Rettig, H. R. Tseng, C. Shao and E. M. Posadas, *Methods*, 2013, **64**, 144–152.

134 A. Abdulla, T. Zhang, S. Li, W. Guo, A. R. Warden, Y. Xin, N. Maboyi, J. Lou, H. Xie and X. Ding, *Microsyst. Nanoeng.*, 2022, **8**, 13.

135 F. D. Schwab, M. C. Scheidmann, L. L. Ozimski, A. Kling, L. Armbrecht, T. Ryser, I. Krol, K. Strittmatter, B. D. Nguyen-Sträuli, F. Jacob, A. Fedier, V. Heinzelmann-Schwarz, A. Wicki, P. S. Dittrich and N. Aceto, *Microsyst. Nanoeng.*, 2022, **8**, 130.

136 S. H. Au, J. Edd, A. E. Stoddard, K. H. K. Wong, F. Fachin, S. Maheswaran, D. A. Haber, S. L. Stott, R. Kapur and M. Toner, *Sci. Rep.*, 2017, **7**, 2433.



137 S. C. Hur, A. J. Mach and D. Di Carlo, *Biomicrofluidics*, 2011, **5**, 022206.

138 S. L. Stott, C.-H. Hsu, D. I. Tsukrov, M. Yu, D. T. Miyamoto, B. A. Waltman, S. M. Rothenberg, A. M. Shah, M. E. Smas, G. K. Korir, F. P. Floyd, A. J. Gilman, J. B. Lord, D. Winokur, S. Springer, D. Irimia, S. Nagrath, L. V. Sequist, R. J. Lee, K. J. Isselbacher, S. Maheswaran, D. A. Haber and M. Toner, *Proc. Natl. Acad. Sci. U. S. A.*, 2010, **107**, 18392–18397.

139 N. Xiang, J. Wang, Q. Li, Y. Han, D. Huang and Z. Ni, *Anal. Chem.*, 2019, **91**, 10328–10334.

140 S. Nagrath, L. V. Sequist, S. Maheswaran, D. W. Bell, D. Irimia, L. Ulkus, M. R. Smith, E. L. Kwak, S. Digumarthy, A. Muzikansky, P. Ryan, U. J. Balis, R. G. Tompkins, D. A. Haber and M. Toner, *Nature*, 2007, **450**, 1235–1239.

141 J. P. Gleghorn, E. D. Pratt, D. Denning, H. Liu, N. H. Bander, S. T. Tagawa, D. M. Nanus, P. A. Giannakakou and B. J. Kirby, *Lab Chip*, 2010, **10**, 27–29.

142 H. J. Yoon, T. H. Kim, Z. Zhang, E. Azizi, T. M. Pham, C. Paoletti, J. Lin, N. Ramnath, M. S. Wicha, D. F. Hayes, D. M. Simeone and S. Nagrath, *Nat. Nanotechnol.*, 2013, **8**, 735–741.

143 Y. H. Cheng, Y. C. Chen, E. Lin, R. Brien, S. Jung, Y. T. Chen, W. Lee, Z. Hao, S. Sahoo, H. Min Kang, J. Cong, M. Burness, S. Nagrath, M. S. Wicha and E. Yoon, *Nat. Commun.*, 2019, **10**, 2163.

144 F. Olm, A. Urbansky, J. H. Dykes, T. Laurell and S. Scheding, *Sci. Rep.*, 2019, **9**, 8777.

145 M. Labib, Z. Wang, S. U. Ahmed, R. M. Mohamadi, B. Duong, B. Green, E. H. Sargent and S. O. Kelley, *Nat. Biomed. Eng.*, 2021, **5**, 41–52.

146 C. H. Chu, R. Liu, T. Ozkaya-Ahmador, M. Boya, B. E. Swain, J. M. Owens, E. Burentugs, M. A. Bilen, J. F. McDonald and A. F. Sarioglu, *Lab Chip*, 2019, **19**, 3427–3437.

147 F. Fachin, P. Spuhler, J. M. Martel-Foley, J. F. Edd, T. A. Barber, J. Walsh, M. Karabacak, V. Pai, M. Yu, K. Smith, H. Hwang, J. Yang, S. Shah, R. Yarmush, L. V. Sequist, S. L. Stott, S. Maheswaran, D. A. Haber, R. Kapur and M. Toner, *Sci. Rep.*, 2017, **7**, 10936.

148 Z. Liu, Y. Huang, W. Liang, J. Bai, H. Feng, Z. Fang, G. Tian, Y. Zhu, H. Zhang, Y. Wang, A. Liu and Y. Chen, *Lab Chip*, 2021, **21**, 2281–2891, DOI: [10.1039/D1LC00360G](https://doi.org/10.1039/D1LC00360G).

149 J. F. Edd, A. Mishra, T. D. Dubash, S. Herrera, R. Mohammad, E. K. Williams, X. Hong, B. R. Mutlu, J. R. Walsh, F. Machado de Carvalho, B. Aldikacti, L. T. Nieman, S. L. Stott, R. Kapur, S. Maheswaran, D. A. Haber and M. Toner, *Lab Chip*, 2020, **20**, 558–567.

150 M. Dhar, E. Pao, C. Renier, D. E. Go, J. Che, R. Montoya, R. Conrad, M. Matsumoto, K. Heirich, M. Triboulet, J. Rao, S. S. Jeffrey, E. B. Garon, J. Goldman, N. P. Rao, R. Kulkarni, E. Sollier-Christen and D. Di Carlo, *Sci. Rep.*, 2016, **6**, 35474.

151 S. J. Tan, L. Yobas, G. Y. H. Lee, C. N. Ong and C. T. Lim, *Biomed. Microdevices*, 2009, **11**, 883–892.

152 T.-H. Kim, M. Lim, J. Park, J. M. Oh, H. Kim, H. Jeong, S. J. Lee, H. C. Park, S. Jung, B. C. Kim, K. Lee, M.-H. Kim, D. Y. Park, G. H. Kim and Y.-K. Cho, *Anal. Chem.*, 2017, **89**, 1155–1162.

153 A. Lee, J. Park, M. Lim, V. Sunkara, S. Y. Kim, G. H. Kim, M.-H. Kim and Y.-K. Cho, *Anal. Chem.*, 2014, **86**, 11349–11356.

154 J.-M. Park, M. S. Kim, H.-S. Moon, C. E. Yoo, D. Park, Y. J. Kim, K.-Y. Han, J.-Y. Lee, J. H. Oh, S. S. Kim, W.-Y. Park, W.-Y. Lee and N. Huh, *Anal. Chem.*, 2014, **86**, 3735–3742.

155 J. Zhou, A. Kulasinghe, A. Bogseth, K. O'Byrne, C. Punyadeera and I. Papautsky, *Microsyst. Nanoeng.*, 2019, **5**, 8.

156 H. W. Hou, M. E. Warkiani, B. L. Khoo, Z. R. Li, R. A. Soo, D. S.-W. Tan, W.-T. Lim, J. Han, A. A. S. Bhagat and C. T. Lim, *Sci. Rep.*, 2013, **3**, 1259.

157 A. Kulasinghe, J. Zhou, L. Kenny, I. Papautsky and C. Punyadeera, *Cancers*, 2019, **11**, 89, DOI: [10.3390/cancers11010089](https://doi.org/10.3390/cancers11010089).

158 M.-D. Chen, Y.-T. Yang, Z.-Y. Deng, H.-Y. Xu, J.-N. Deng, Z. Yang, N. Hu and J. Yang, *Chin. J. Anal. Chem.*, 2019, **47**, 661–668.

159 P. C. Chen, C. C. Chen and K. C. Young, *Biomicrofluidics*, 2016, **10**, 054112.

160 X. Su, J. Zhang, D. Zhang, Y. Wang, M. Chen, Z. Weng, J. Wang, J. Zeng, Y. Zhang, S. Zhang, S. Ge, J. Zhang and N. Xia, *Micromachines*, 2020, **11**, 352, DOI: [10.3390/mi11040352](https://doi.org/10.3390/mi11040352).

161 Y. Nakashima, S. Hata and T. Yasuda, *Sens. Actuators, B*, 2010, **145**, 561–569.

162 A. Piovesan, M. C. Pelleri, F. Antonaros, P. Strippoli, M. Caracausi and L. Vitale, *BMC Res. Notes*, 2019, **12**, 106.

163 L. R. Huang, E. C. Cox, R. H. Austin and J. C. Sturm, *Science*, 2004, **304**, 987–990.

164 R. Vernekar, T. Kruger, K. Loutherback, K. Morton and D. W. Inglis, *Lab Chip*, 2017, **17**, 3318–3330.

165 S. H. Au, J. Edd, A. E. Stoddard, K. H. K. Wong, F. Fachin, S. Maheswaran, D. A. Haber, S. L. Stott, R. Kapur and M. Toner, *Sci. Rep.*, 2017, **7**, 2433.

166 T. Ohnaga, Y. Takei, T. Nagata and Y. Shimada, *Sci. Rep.*, 2018, **8**, 12005.

167 S. Merugu, L. Chen, E. Gavens, H. Gabra, M. Brougham, G. Makin, A. Ng, D. Murphy, A. S. Gabriel, M. L. Robinson, J. H. Wright, S. A. Burchill, A. Humphreys, N. Bown, D. Jamieson and D. A. Tweddle, *Clin. Cancer Res.*, 2020, **26**, 122.

168 F. Rifatbegovic, C. Frech, M. R. Abbasi, S. Taschner-Mandl, T. Weiss, W. M. Schmidt, I. Schmidt, R. Ladenstein, I. M. Ambros and P. F. Ambros, *Int. J. Cancer*, 2018, **142**, 297–307.

169 H. Scharpenseel, A. Hanssen, S. Loges, M. Mohme, C. Bernreuther, S. Peine, K. Lamszus, Y. Goy, C. Petersen, M. Westphal, M. Glatzel, S. Riethdorf, K. Pantel and H. Wilkman, *Sci. Rep.*, 2019, **9**, 7406–7406.

170 G. Galletti, M. S. Sung, L. T. Vahdat, M. A. Shah, S. M. Santana, G. Altavilla, B. J. Kirby and P. Giannakakou, *Lab Chip*, 2014, **14**, 147–156.



171 R. Königsberg, E. Obermayr, G. Bises, G. Pfeiler, M. Gneist, F. Wrba, M. de Santis, R. Zeillinger, M. Hudec and C. Dittrich, *Acta Oncol.*, 2011, **50**, 700–710.

172 X. Liu, Z. Zhang, B. Zhang, Y. Zheng, C. Zheng, B. Liu, S. Zheng, K. Dong and R. Dong, *EBioMedicine*, 2018, **35**, 244–250.

173 S. G. Dubois, C. L. Epling, J. Teague, K. K. Matthay and E. Sinclair, *Pediatr. Blood Cancer*, 2010, **54**, 13–18.

174 K. A. Hyun, G. B. Koo, H. Han, J. Sohn, W. Choi, S. I. Kim, H. I. Jung and Y. S. Kim, *Onco Targets Ther.*, 2016, **7**, 24677–24687.

175 F. Le Du, T. Fujii, K. Kida, D. W. Davis, M. Park, D. D. Liu, W. Wu, M. Chavez-MacGregor, C. H. Barcenas, V. Valero, D. Tripathy, J. M. Reuben and N. T. Ueno, *PLoS One*, 2020, **15**, e0229903.

176 J. Kitz, D. Goodale, C. Postenka, L. E. Lowes and A. L. Allan, *Clin. Exp. Metastasis*, 2021, **38**, 97–108.

177 T. M. Gorges, I. Tinhofer, M. Drosch, L. Rose, T. M. Zollner, T. Krahn and O. von Ahsen, *BMC Cancer*, 2012, **12**, 178.

178 C. G. Rao, D. Chianese, G. V. Doyle, M. C. Miller, T. Russell, R. A. Sanders, Jr. and L. W. Terstappen, *Int. J. Oncol.*, 2005, **27**, 49–57.

179 A. Markiewicz, J. Topa, A. Nagel, J. Skokowski, B. Seroczynska, T. Stokowy, M. Welnicka-Jaskiewicz and A. J. Zaczek, *Cancers*, 2019, **11**, 59, DOI: [10.3390/cancers11010059](https://doi.org/10.3390/cancers11010059).

180 S. Mukherjee, T. G. Kang, Y. Chen and S. Kim, *Crit. Rev. Biomed. Eng.*, 2009, **37**, 517–529.

181 D. A. Fedosov, B. Caswell, A. S. Popel and G. E. Karniadakis, *Microcirculation*, 2010, **17**, 615–628.

182 S. Tripathi, Y. V. B. Varun Kumar, A. Prabhakar, S. S. Joshi and A. Agrawal, *J. Micromech. Microeng.*, 2015, **25**, 083001.

183 X. Xue, M. K. Patel, M. Kersaudy-Kerhoas, M. P. Y. Desmulliez, C. Bailey and D. Topham, *Appl. Math. Model.*, 2012, **36**, 743–755.

184 S. Yang, A. Ündar and J. D. Zahn, *Lab Chip*, 2006, **6**, 871–880.

185 X. Li, A. S. Popel and G. E. Karniadakis, *Phys. Biol.*, 2012, **9**, 026010–026010.

186 R. D. Jäggi, R. Sandoz and C. S. Effenhauser, *Microfluid. Nanofluid.*, 2007, **3**, 47–53.

187 M. Kersaudy-Kerhoas, R. Dhariwal, M. P. Y. Desmulliez and L. Jouvet, *Microfluid. Nanofluid.*, 2009, **8**, 105.

188 D. Di Carlo, D. Irimia, R. G. Tompkins and M. Toner, *Proc. Natl. Acad. Sci. U. S. A.*, 2007, **104**, 18892–18897.

189 D. Di Carlo, *Lab Chip*, 2009, **9**, 3038–3046.

190 A. A. S. Bhagat, S. S. Kuntaegowdanahalli and I. Papautsky, *Microfluid. Nanofluid.*, 2009, **7**, 217–226.

191 H. Amini, W. Lee and D. Di Carlo, *Lab Chip*, 2014, **14**, 2739–2761.

192 S. Razavi Bazaz, A. Mihandust, R. Salomon, H. A. N. Joushani, W. Li, H. A. Amiri, F. Mirakhorli, S. Zhand, J. Shrestha, M. Miansari, B. Thierry, D. Jin and M. Ebrahimi Warkiani, *Lab Chip*, 2022, **22**, 4093–4109.

193 J. Seo, M. H. Lean and A. Kole, *J. Chromatogr. A*, 2007, **1162**, 126–131.

194 A. A. S. Bhagat, S. S. Kuntaegowdanahalli and I. Papautsky, *Lab Chip*, 2008, **8**, 1906–1914.

195 T. H. Kim, H. J. Yoon, P. Stella and S. Nagrath, *Biomicrofluidics*, 2014, **8**, 064117.

196 M. Robinson, H. Marks, T. Hinsdale, K. Maitland and G. Cote, *Biomicrofluidics*, 2017, **11**, 024109.

197 E. Lin, L. Rivera-Báez, S. Fouladdel, H. J. Yoon, S. Guthrie, J. Wieger, Y. Deol, E. Keller, V. Sahai, D. M. Simeone, M. L. Burness, E. Azizi, M. S. Wicha and S. Nagrath, *Cell Syst.*, 2017, **5**, 295–304.e294.

198 S. Wan, T. H. Kim, K. J. Smith, R. Delaney, G. S. Park, H. Guo, E. Lin, T. Plegue, N. Kuo, J. Steffes, C. Leu, D. M. Simeone, N. Razimulava, N. D. Parikh, S. Nagrath and T. H. Welling, *Sci. Rep.*, 2019, **9**, 18575.

199 M. Rafeie, J. Zhang, M. Asadnia, W. Li and M. E. Warkiani, *Lab Chip*, 2016, **16**, 2791–2802.

200 J. Sun, M. Li, C. Liu, Y. Zhang, D. Liu, W. Liu, G. Hu and X. Jiang, *Lab Chip*, 2012, **12**, 3952–3960.

201 H. Chen, *Sci. Rep.*, 2018, **8**, 4042.

202 S. Shen, C. Tian, T. Li, J. Xu, S.-W. Chen, Q. Tu, M.-S. Yuan, W. Liu and J. Wang, *Lab Chip*, 2017, **17**, 3578–3591.

203 B. Miller, M. Jimenez and H. Bridle, *Sci. Rep.*, 2016, **6**, 36386.

204 M. G. Lee, J. H. Shin, C. Y. Bae, S. Choi and J.-K. Park, *Anal. Chem.*, 2013, **85**, 6213–6218.

205 M. Zuvin, N. Mansur, S. Z. Birol, L. Trabzon and A. Sayı Yazgan, *Microsyst. Technol.*, 2016, **22**, 645–652.

206 A. S. Rzhevskiy, S. Razavi Bazaz, L. Ding, A. Kapitannikova, N. Sayyadi, D. Campbell, B. Walsh, D. Gillatt, M. Ebrahimi Warkiani and A. V. Zvyagin, *Cancers*, 2019, **12**, 81.

207 B. L. Khoo, M. E. Warkiani, D. S.-W. Tan, A. A. S. Bhagat, D. Irwin, D. P. Lau, A. S. Lim, K. H. Lim, S. S. Krisna and W.-T. Lim, *PLoS One*, 2014, **9**, e99409.

208 S. Park, R. R. Ang, S. P. Duffy, J. Bazov, K. N. Chi, P. C. Black and H. Ma, *PLoS One*, 2014, **9**, e85264–e85264.

209 P. A. J. Mendelaar, J. Kraan, M. Van, L. L. Zeune, L. Terstappen, E. Oomen-de Hoop, J. W. M. Martens and S. Sleijfer, *Mol. Oncol.*, 2021, **15**, 116–125.

210 M. C. Zalis, J. F. Reyes, P. Augustsson, S. Holmqvist, L. Roybon, T. Laurell and T. Deierborg, *Integr. Biol.*, 2016, **8**, 332–340.

211 L. Clime, J. Daoud, D. Brassard, L. Malic, M. Geissler and T. Veres, *Microfluid. Nanofluid.*, 2019, **23**, 29.

212 S. Haeberle, T. Brenner, R. Zengerle and J. Ducrée, *Lab Chip*, 2006, **6**, 776–781.

213 J.-N. Kuo and B.-S. Li, *Biomed. Microdevices*, 2014, **16**, 549–558.

214 J.-N. Kuo and X.-F. Chen, *Microsyst. Technol.*, 2015, **21**, 2485–2494.

215 Y. Shi, P. Ye, K. Yang, B. Qiaoge, J. Xie, J. Guo, C. Wang, Z. Pan, S. Liu and J. Guo, *Electrophoresis*, 2022, **43**, 2250–2259.

216 K. D. Lenz, S. Jakhar, J. W. Chen, A. S. Anderson, D. C. Purcell, M. O. Ishak, J. F. Harris, L. E. Akhakov, J. Z. Kubicek-Sutherland, P. Nath and H. Mukundan, *Sci. Rep.*, 2021, **11**, 5287.



217 A. Hatami, M. Saadatmand and M. Garshasbi, *Talanta*, 2024, **267**, 125245.

218 A. Shamloo, A. Naghdloo and M. Besanjideh, *Sci. Rep.*, 2021, **11**, 1939.

219 C.-C. Lin, J.-C. Tsai, Y.-Z. Liu and J.-N. Kuo, *Microfluid. Nanofluid.*, 2024, **28**, 10.

220 S. Gupta and A. Bit, in *Bioelectronics and Medical Devices*, ed. K. Pal, H.-B. Kraatz, A. Khasnobish, S. Bag, I. Banerjee and U. Kuruganti, Woodhead Publishing, 2019, pp. 123–144, DOI: [10.1016/B978-0-08-102420-1.00008-X](https://doi.org/10.1016/B978-0-08-102420-1.00008-X).

221 M. Wu, A. Ozcelik, J. Rufo, Z. Wang, R. Fang and T. Jun Huang, *Microsyst. Nanoeng.*, 2019, **5**, 32.

222 W. L. Ung, K. Mutafopoulos, P. Spink, R. W. Rambach, T. Franke and D. A. Weitz, *Lab Chip*, 2017, **17**, 4059–4069.

223 T. Franke, A. R. Abate, D. A. Weitz and A. Wixforth, *Lab Chip*, 2009, **9**, 2625–2627.

224 G. Destgeer, B. H. Ha, J. Park, J. H. Jung, A. Alazzam and H. J. Sung, *Phys. Procedia*, 2015, **70**, 34–37.

225 A. Lenshof, C. Magnusson and T. Laurell, *Lab Chip*, 2012, **12**, 1210–1223.

226 T. Laurell, F. Petersson and A. Nilsson, *Chem. Soc. Rev.*, 2007, **36**, 492–506.

227 F. Petersson, L. Åberg, A.-M. Swärd-Nilsson and T. Laurell, *Anal. Chem.*, 2007, **79**, 5117–5123.

228 P. Li, Z. Mao, Z. Peng, L. Zhou, Y. Chen, P.-H. Huang, C. I. Truica, J. J. Drabick, W. S. El-Deiry, M. Dao, S. Suresh and T. J. Huang, *Proc. Natl. Acad. Sci. U. S. A.*, 2015, **112**, 4970.

229 J. Shi, H. Huang, Z. Stratton, Y. Huang and T. J. Huang, *Lab Chip*, 2009, **9**, 3354–3359.

230 F. Petersson, A. Nilsson, H. Jönsson and T. Laurell, *Anal. Chem.*, 2005, **77**, 1216–1221.

231 P. Augustsson, C. Magnusson, M. Nordin, H. Lilja and T. Laurell, *Anal. Chem.*, 2012, **84**, 7954–7962.

232 M. Wu, Y. Ouyang, Z. Wang, R. Zhang, P.-H. Huang, C. Chen, H. Li, P. Li, D. Quinn, M. Dao, S. Suresh, Y. Sadovsky and T. J. Huang, *Proc. Natl. Acad. Sci. U. S. A.*, 2017, **114**, 10584.

233 J. Dykes, A. Lenshof, I.-B. Åstrand-Grundström, T. Laurell and S. Scheding, *PLoS One*, 2011, **6**, e23074.

234 J. Nam, H. Lim, D. Kim and S. Shin, *Lab Chip*, 2011, **11**, 3361–3364.

235 Y. Chen, M. Wu, L. Ren, J. Liu, P. H. Whitley, L. Wang and T. J. Huang, *Lab Chip*, 2016, **16**, 3466–3472.

236 C. Magnusson, P. Augustsson, A. Lenshof, Y. Ceder, T. Laurell and H. Lilja, *Anal. Chem.*, 2017, **89**, 11954–11961.

237 M. Antfolk, C. Antfolk, H. Lilja, T. Laurell and P. Augustsson, *Lab Chip*, 2015, **15**, 2102–2109.

238 M. Wu, P. H. Huang, R. Zhang, Z. Mao, C. Chen, G. Kemeny, P. Li, A. V. Lee, R. Gyanchandani, A. J. Armstrong, M. Dao, S. Suresh and T. J. Huang, *Small*, 2018, **14**, e1801131.

239 A. Mishra, T. D. Dubash, J. F. Edd, M. K. Jewett, S. G. Garre, N. M. Karabacak, D. C. Rabe, B. R. Mutlu, J. R. Walsh, R. Kapur, S. L. Stott, S. Maheswaran, D. A. Haber and M. Toner, *Proc. Natl. Acad. Sci. U. S. A.*, 2020, **117**, 16839–16847.

240 R. Hulspas, L. Villa-Komaroff, E. Koksal, K. Etienne, P. Rogers, M. Tuttle, O. Korsgren, J. C. Sharpe and D. Berglund, *Cyotherapy*, 2014, **16**, 1384–1389.

241 T.-H. Wu, Y. Chen, S.-Y. Park, J. Hong, T. Teslaa, J. F. Zhong, D. Di Carlo, M. A. Teitell and P.-Y. Chiou, *Lab Chip*, 2012, **12**, 1378–1383.

242 K. Mutafopoulos, P. Spink, C. D. Lofstrom, P. J. Lu, H. Lu, J. C. Sharpe, T. Franke and D. A. Weitz, *Lab Chip*, 2019, **19**, 2435–2443.

243 C. H. Chen, S. H. Cho, F. Tsai, A. Erten and Y.-H. Lo, *Biomed. Microdevices*, 2009, **11**, 1223.

244 S. Sakuma, Y. Kasai, T. Hayakawa and F. Arai, *Lab Chip*, 2017, **17**, 2760–2767.

245 A. Isozaki, H. Mikami, H. Tezuka, H. Matsumura, K. Huang, M. Akamine, K. Hiramatsu, T. Iino, T. Ito, H. Karakawa, Y. Kasai, Y. Li, Y. Nakagawa, S. Ohnuki, T. Ota, Y. Qian, S. Sakuma, T. Sekiya, Y. Shirasaki, N. Suzuki, E. Tayyabi, T. Wakamiya, M. Xu, M. Yamagishi, H. Yan, Q. Yu, S. Yan, D. Yuan, W. Zhang, Y. Zhao, F. Arai, R. E. Campbell, C. Danelon, D. Di Carlo, K. Hiraki, Y. Hoshino, Y. Hosokawa, M. Inaba, A. Nakagawa, Y. Ohya, M. Oikawa, S. Uemura, Y. Ozeki, T. Sugimura, N. Nitta and K. Goda, *Lab Chip*, 2020, **20**, 2263–2273.

246 T. Franke, S. Braunmuller, L. Schmid, A. Wixforth and D. A. Weitz, *Lab Chip*, 2010, **10**, 789–794.

247 L. Schmid, D. A. Weitz and T. Franke, *Lab Chip*, 2014, **14**, 3710–3718.

248 D. J. Collins, A. Neild and Y. Ai, *Lab Chip*, 2016, **16**, 471–479.

249 C. W. T. Shields, C. D. Reyes and G. P. Lopez, *Lab Chip*, 2015, **15**, 1230–1249.

250 J. Voldman, *Annu. Rev. Biomed. Eng.*, 2006, **8**, 425–454.

251 K. Takahashi, A. Hattori, I. Suzuki, T. Ichiki and K. Yasuda, *J. Nanobiotechnol.*, 2004, **2**, 5.

252 P. S. Dittrich, M. Jahnz and P. Schwille, *ChemBioChem*, 2005, **6**, 811–814.

253 L. Shang, Y. Cheng and Y. Zhao, *Chem. Rev.*, 2017, **117**, 7964–8040.

254 J. C. Baret, O. J. Miller, V. Taly, M. Ryckelynck, A. El-Harrak, L. Frenz, C. Rick, M. L. Samuels, J. B. Hutchison, J. J. Agresti, D. R. Link, D. A. Weitz and A. D. Griffiths, *Lab Chip*, 2009, **9**, 1850–1858.

255 A. Sciambi and A. R. Abate, *Lab Chip*, 2015, **15**, 47–51.

256 L. Mazutis, J. Gilbert, W. L. Ung, D. A. Weitz, A. D. Griffiths and J. A. Heyman, *Nat. Protoc.*, 2013, **8**, 870–891.

257 O. D. Velev and K. H. Bhatt, *Soft Matter*, 2006, **2**, 738–750.

258 A. Y. Fu, C. Spence, A. Scherer, F. H. Arnold and S. R. Quake, *Nat. Biotechnol.*, 1999, **17**, 1109–1111.

259 P. G. Erlandsson and N. D. Robinson, *Electrophoresis*, 2011, **32**, 784–790.

